David Publishing Company
www.davidpublisher.com

ISSN 2162-5263 (Print)
ISSN 2162-5271 (Online)
DOI:10.17265/2162-5263

Journal of Environmental Science and Engineering B

Volume 7, Number 3, March 2018

From Knowledge to Wisdom

Journal of Environmental Science and Engineering B

Volume 7, Number 3, March 2018 (Serial Number 69)

David Publishing Company
www.davidpublisher.com

Publication Information:
Journal of Environmental Science and Engineering B (formerly parts of Journal of Environmental Science and Engineering ISSN 1934-8932, USA) is published monthly in hard copy (ISSN 2162-5263) and online (ISSN 2162-5271) by David Publishing Company located at 616 Corporate Way, Suite 2-4876, Valley Cottage, NY 10989, USA.

Aims and Scope:
Journal of Environmental Science and Engineering B, a monthly professional academic journal, covers all sorts of researches on environmental management and assessment, environmental monitoring, atmospheric environment, aquatic environment and municipal solid waste, etc..

Manuscripts and correspondence are invited for publication. You can submit your papers via Web Submission, or E-mail to environmental@davidpublishing.com, environmental@davidpublishing.org or info@davidpublishing.org. Submission guidelines and Web Submission system are available at http://www.davidpublisher.com.

Editorial Office:
616 Corporate Way, Suite 2-4876, Valley Cottage, NY 10989, USA
Tel: 1-323-984-7526, 323-410-1082
Fax: 1-323-984-7374, 323-908-0457
E-mail: environmental@davidpublishing.com; environmental@davidpublishing.org; info@davidpublishing.org

Abstracted/Indexed in:
Google Scholar
CAS (Chemical Abstracts Service)
Database of EBSCO, Massachusetts, USA
Chinese Database of CEPS, Airiti Inc. & OCLC
Cambridge Science Abstracts (CSA)
Ulrich's Periodicals Directory
Chinese Scientific Journals Database, VIP Corporation, Chongqing, China
Summon Serials Solutions
Proquest

Subscription Information:
Price (per year):
Print $600, Online $480
Print and Online $800

David Publishing Company
616 Corporate Way, Suite 2-4876, Valley Cottage, NY 10989, USA
Tel: 1-323-984-7526, 323-410-1082; Fax: 1-323-984-7374, 323-908-0457
E-mail: order@davidpublishing.com
Digital Cooperative Company: www.bookan.com.cn

David Publishing Company
www.davidpublisher.com

Journal of Environmental Science and Engineering B

Volume 7, Number 3, March 2018 (Serial Number 69)

Contents

Journal of Environmental Science and Engineering B 7 (2018) 83-91
doi:10.17265/2162-5263/2018.03.001

Execution of Measurements for Determining the Parameters Affecting the Thermochemical Treatment of Brine Treated Biomass and the Adsorption of Dyes

Odysseas Kopsidas

Department of Industrial Management and Technology, University of Piraeus, Piraeus 18534, Greece

Abstract: Brine is a solution of salt (usually sodium chloride) in water. In different contexts, brine may refer to salt solutions ranging from about 3.5% (a typical concentration of seawater, or the lower end of solutions used for brining foods) up to about 26% (a typical saturated solution, depending on temperature). Adsorption onto activated carbon is the most widespread technology for the removal of pollutants from water and wastewaters. In this study, continuous fixed-bed-column systems were investigated. The adsorbents which authors use are: spruce (*Picea abies*) untreated, spruce modified by autohydrolysis. The column systems were filed with biomass at various initial dye concentrations, flow rates and bed-depths. The column kinetics of MB (Methylene Blue) adsorption on spruce (*Picea abies*) untreated, spruce modified by autohydrolysis was simulated. Economies arise when the facility that can use such adsorption materials is near a source of a lignocellulosic waste as agricultural residues, thus saving transportation cost and contributing to industrial ecology at local level.

Key words: Adsorption, desorption, column studies, pretreatment, brine.

1. Introduction

Brine is a solution of salt (usually sodium chloride) in water. In different contexts, brine may refer to salt solutions ranging from about 3.5% (a typical concentration of seawater, or the lower end of solutions used for brining foods) up to about 26% (a typical saturated solution, depending on temperature). Brine is a liquid, and 0 °F was initially set as the zero point in the Fahrenheit temperature scale, as it was the coldest temperature that Daniel Gabriel Fahrenheit could reliably reproduce—by freezing brine. At 100 °C (373.65 K, 212 °F), saturated sodium chloride brine is about 28% salt by weight i.e. 39.12 g salt dissolves in 100 mL of water at 100 °C. At 0 °C (273.15 K, 32 °F), brine can only hold about 26% salt. Brine is a common fluid used in large refrigeration installations for the transport of thermal energy from place to place. It is used because the addition of salt to water lowers the freezing temperature of the solution and the heat transport efficiency can be greatly enhanced for the comparatively low cost of the material. The lowest freezing point obtainable for NaCl brine is -21.1 °C (-6.0 °F) at 23.3wt% NaCl. This is called the eutectic point [1, 2]. According to many review papers [3-8], low-cost adsorbents offer a lot of promising benefits for commercial purposes in the future. They could be used in place of commercial activated carbon for the removal of dyes in aqueous solutions.

Adsorption onto activated carbon is the most widespread technology for the removal of pollutants from water and wastewaters. The disadvantage of activated carbon is its high cost [11]. Hence, it is of pivotal importance thence of low-cost substitute absorbents to replace activated carbons. Various types of untreated biomass have been reported to have a use in dye removal: sawdust [9, 11], wheat straw [12], cedar sawdust [13], rubberwood sawdust [14], kudzu [15], banana and orange peels [16] and palm kernel

Corresponding author: Odysseas Kopsidas, Ph.D., research fields: environmental economics.

fiber [11, 17], peanut husk [4], palm kernel fibre [11], *Turbinaria turbinate* alga [12], graphene [13], defatted jojoba [14] and sugar bet pulp [15].

Further, numerous pretreated lignocellulosic materials are used to remove dyes in water and wastewater: Pyrolyzed date pits [16], date stones [17] and *Turbinaria turbinate* alga.

In this study, continuous fixed-bed-column systems were investigated. The adsorbents which authors use are: spruce (*Picea abies*) untreated and spruce modified by brine treatment. The column systems were filed with biomass at various initial dye concentrations, flow rates and bed-depths. The column kinetics of MB (Methylene Blue) adsorption on spruce (*Picea abies*) untreated, and spruce modified by brine treatment, was simulated herein, using biomass as control, in order to facilitate its potential use as a low cost adsorbent for wastewater dye removal. Economies arise when the facility that can use such adsorption materials is near a source of a lignocellulosic waste as agricultural residues, thus saving transportation cost and contributing to industrial ecology at local level.

2. Materials and Methods

The brine treatment process was performed in a 3.75-L batch reactor PARR 4843. The isothermal autohydrolysis time was tai = 0, 10, 20, 30, 40 and 50 min (not including the non-isothermal preheating and the cooling time-periods); the reaction was catalyzed by the organic acids produced by the pine sawdust itself during autohydrolysis at a liquid-to-solid ratio of 10:1; the liquid phase volume (water) was 2,000 mL and the solid material dose (pine sawdust) was 200 g; stirring speed 150 rpm. The reaction ending temperature values were T = 160 °C, 200 °C and 240 °C, reached after t = 42, 62 and 80 min preheating time values, respectively. The autohydrolysis product was filtered using a Buchner filter with Munktell paper sheet (grade 34/N) to separate the liquid phase and from the solid phase. The solid residue was washed with water until neutral pH (the initial filtrate pH was 2.90-4.76 depending on the autohydrolysis severity). The solid residue was dried at 110 °C for 10 days at room temperature to reach the humidity of the untreated material. Then it was used as adsorbent.

Continue-flow experiments were carried out on stainless steel columns with dimensions 15 × 2.5 cm. The bed height was x = 15 cm, respectively. The adsorbent weight was m = 32 g and 54 g, respectively. The pH was 8.0. The flow rates were fixed at approximately 20 mL·min^{-1} using a preparative HPLC (High Performance Liquid Chromatography) pump, LaPrep P110-VWR-VWR International. The initial concentrations of MB were 165 mg·L^{-1}. To determine the concentration of MB in the effluent, samples of outflow were peaked at 100 mL intervals.

3. Results and Discussion

A widely used continuous fixed-bed-column model was established by Bohart and Adams [17], who assumed that the rate of adsorption is controlled by the surface binding (through chemical reaction or physical interaction) between adsorbate and unused capacity of the solid, i.e., adsorption rate = $K \cdot C \cdot C_u$, where K is the adsorption rate coefficient, C is the adsorbate concentration at the solid phase at distance x, and C_u is the unused surface adsorptive capacity at time t, expressed as mass per volume of bed. The material balance for adsorbate is given by the partial differential equation:

$$\frac{\partial C_u}{\partial t} = -K \cdot C \cdot C_u \quad (1)$$

while the corresponding partial differential equation for the C_u decrease is

$$\frac{\partial C}{\partial x} = -\frac{K}{u} \cdot C \cdot C_u \quad (2)$$

where u is the superficial liquid velocity. These equations are obtained neglecting diffusion and

accumulation terms, assumptions that are valid in chemical engineering practice, provided that strict scale up specifications are kept in the design stage and successful operation conditions are kept in the industrial operation stage.

The differential equations can be integrated over the total length x of the bed to give:

$$\ln\left(\frac{C_i}{C}-1\right)=\ln[\exp\left(\frac{K.N.x}{u}\right)-1]-K\cdot C_i\cdot t \quad (3)$$

where N (mg·L^{-1}) is the initial or total adsorption capacity coefficient, also quoted as $C_{u,0}$ [17]; C = effluent concentration (mg·L^{-1}); C_i = influent concentration (mg·L^{-1}); K = adsorption rate coefficient ($L\cdot mg^{-1}\cdot min^{-1}$); x = bed depth (cm); u = linear velocity (cm·min^{-1}); and t = time (min). Since $\exp(K.N.x/u)$ is usually much greater than unity, this equation can be simplified to:

$$\ln\left(\frac{C_i}{C}-1\right)=\frac{K\cdot N\cdot x}{u}-K\cdot C_i\cdot t \quad (4)$$

which is commonly used by researchers, because of its convenience in estimating the values of parameters K and N through linear regression either of ln[(C_0/C_i) – 1] vs. t or t vs. x when the following rearrangement is adopted:

$$t=\frac{N\cdot x}{C_i\cdot u}-\frac{1}{K\cdot C_i}\cdot\left(\ln\frac{C_i}{C}-1\right) \quad (5)$$

In this rearrangement, t is the time to breakthrough, i.e., the time period required for concentration to reach a predetermined value. For using the last expression as a linear regression model, wastewater is passed through beds of varying depths, keeping constant C_i and u, preferably at values similar to those expected to prevail under real conditions at full scale. Alternatively, it can be performed by the aid of at least three columns arranged in series. In such a case, sampling takes place at the bottom of each column and is measured for adsorbate concentration, making more frequent measurements when approaching the breakthrough concentration C. Finally, the time at which the effluent reaches this concentration is used as the dependent variable while x plans the role of the independent one. Evidently, the use of such a regression model implies the additional error of measuring the independent variable with less precision in comparison with the dependent. The common error in both models comes from the estimation of concentration from measuring adsorbance although the reference relation/curve has been structured/drawn in the inverse mode, i.e., for predetermined concentrations the corresponding adsorbances have been measured.

In the present work, the model of Eq. (17) has been used for parameter values estimation through linear regression to obtain numerical results comparable with corresponding data found for other fixed bed adsorption studies in literature. The non-linear form of this model is:

$$C=\frac{C_i}{1+Ae^{-rt}} \quad (6)$$

where $A=e^{K\cdot N\cdot x/u}$; $r=K\cdot C_i$.

On the other hand, Clark [18] has advanced the Bohart and Adams model [19] by incorporating the parameter n of the Freundlich adsorption isotherm:

$$C=\left[\frac{C_i^{\,n-1}}{1+Ae^{-rt}}\right]^{\frac{1}{n-1}} \quad (7)$$

where n = inverse of the slope of the Freundlich isotherm [12]. Finally, the Bohart and Adams model can be reduced for n = 2 from Clark model [19].

The kinetic equation used for desorption is Eq. (21):

$$C=C'_0\,e^{-k'\cdot t'} \quad (21)$$

where C'_0 is the initial MB concentration of desorption effluent, k' is desorption rate constant assuming first order desorption kinetics and t' is desorption time.

The use of salt brine—a mixture of 23 percent salt

and 77 percent water (the carrying capacity of slat in a water solution)—for melting snow and ice was developed in Europe. The mixture is sprayed directly on the road as an anti-icing agent. Although salt brine has the same melting characteristics of regular salt, because it is in brine form, it has the advantage of working immediately and does not have the problem of "bouncing and scattering" off the road because of its consistency, according to a study of salt brine use by the Vermont Agency of Transportation, Materials and Research Section. The agency found that brine was cost effective to produce, at about $0.10 per gallon. Additionally, other deicing chemicals can be mixed into the salt brine to lower the effective melting temperature. During the study (Table 1) in which experimental test sections of Vermont interstates were treated with salt brine and salt brine mixtures, the agency found that it saved an average of 24 percent of material usage.

Although the data sets were not as extensive as the research team initially thought, the research project was able to produce salt savings of approximately 30 percent and materials cost savings of approximately 30 percent and materials cost savings of approximately 24 percent during the first year of experimentation, according to the Vermont DOT report. If such a cost saving could be projected statewide, the potential savings would be almost $1 million annually. The research team agreed that there is potential for more salt and cost savings as staff becomes more experienced with the technology (Figs. 1-7).

Table 1 Fixed bed column systems for spruce modified by brine treatment.

Concentrated X Times	*T* (°C)	*t* (min)	*Ci*	*Q* (mL/min)	x (cm)	m (g)	N	K	R	qo (mg/g)
1	180	50	153	18	15	20	4948	0.000353	-0.9481	18.21
2	180	50	145	21	15	20	6975	0.000242	-0.9683	25.67
4	140	0	210	21	15	12.11	8461	0.000153	-0.9616	51.42
4	160	0	156	21	15	11.7	4304	0.000694	-0.9946	27.07
4	160	50	163	21	15	20	5834	0.000300	-0.9662	21.47
4	180	0	162	21	15	11.6	6054	0.000257	-0.9744	38.41
4	180	50	151	21	15	20	5666	0.000444	-0.9479	20.85
4	200	0	155	22	15	12.3	4682	0.000866	-0.9667	28.01
4	200	50	162	21	15	14.6	9259	0.000132	-0.9390	46.67
4	200	50	148	21	15	20	7713	0.000157	-0.9232	28.38
4	220	50	157	21	15	12	5840	0.000235	-0.9863	35.82
4	200	50	160	21	15	20	9233	0.000181	-0.9466	33.97
4	240	50	162	19	15	13	1358	0.000899	-0.9237	7.69
4	240	50	153	21	15	12	451	0.000369	-0.7918	2.76
4	240	50	153	21	15	12	451	0.000369	-0.7918	2.76
8	180	0	169	21	15	12	4715	0.000212	-0.9565	28.92
8	180	50	159	17	15	17.3	7089	0.000351	-0.9211	30.16
8	180	50	141	21	15	20	5695	0.000259	-0.9799	20.96

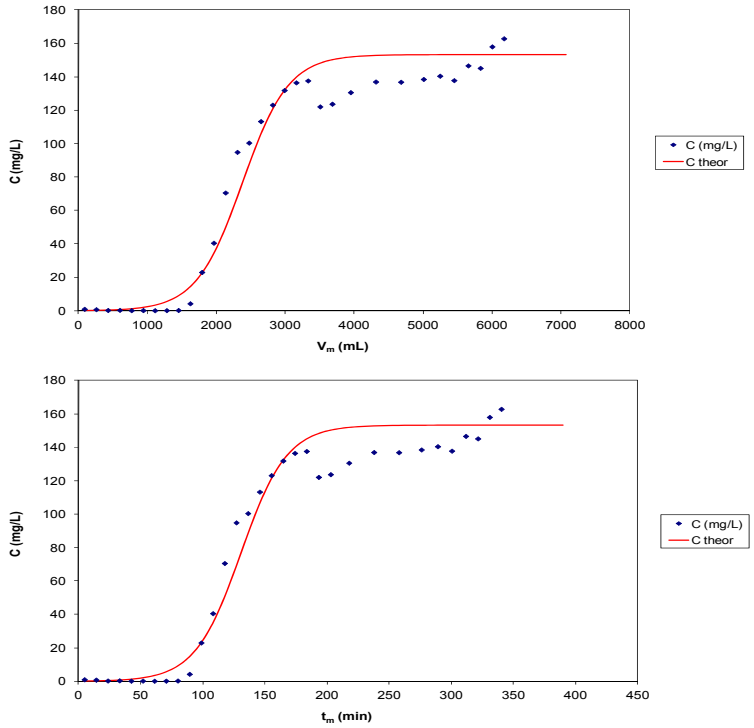

Fig. 1 Column experimental data and theoretical curves of MB adsorption on modified spruce; the effluent concentration is presented vs. (a) the effluent volume and (b) the adsorption time; x = 15 cm, C_i = 160 mg·L^{-1}, Q = 20 mL·min^{-1} (the theoretical curves are according to the Bohart and Adams model); modified by brine treatment; concentrated ×1 time at 180 °C for 50 min.

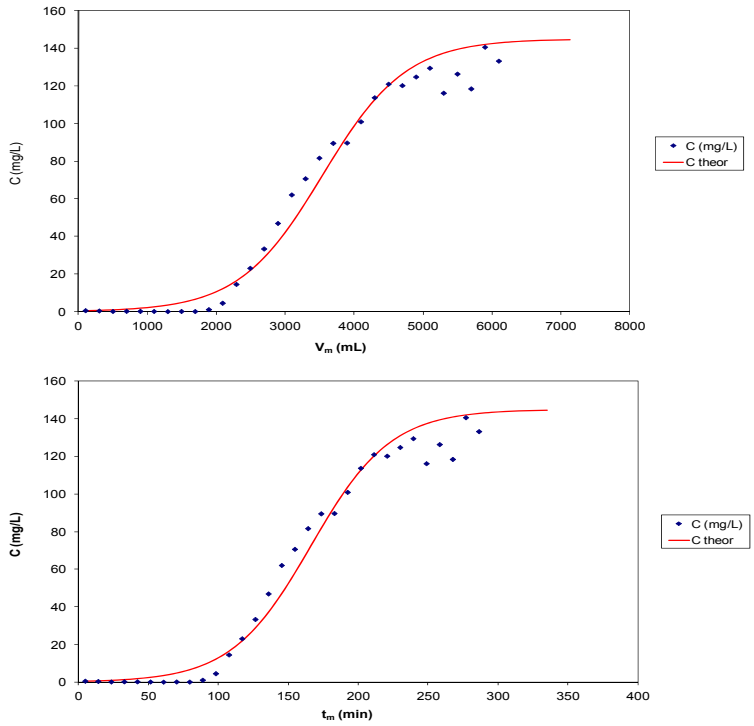

Fig. 2 Column experimental data and theoretical curves of MB adsorption on modified spruce; the effluent concentration is presented vs. (a) the effluent volume and (b) the adsorption time; x = 15 cm, C_i = 160 mg·L^{-1}, Q = 20 mL·min^{-1} (the theoretical curves are according to the Bohart and Adams model); modified by brine treatment; concentrated ×2 times at 180 °C for 50 min.

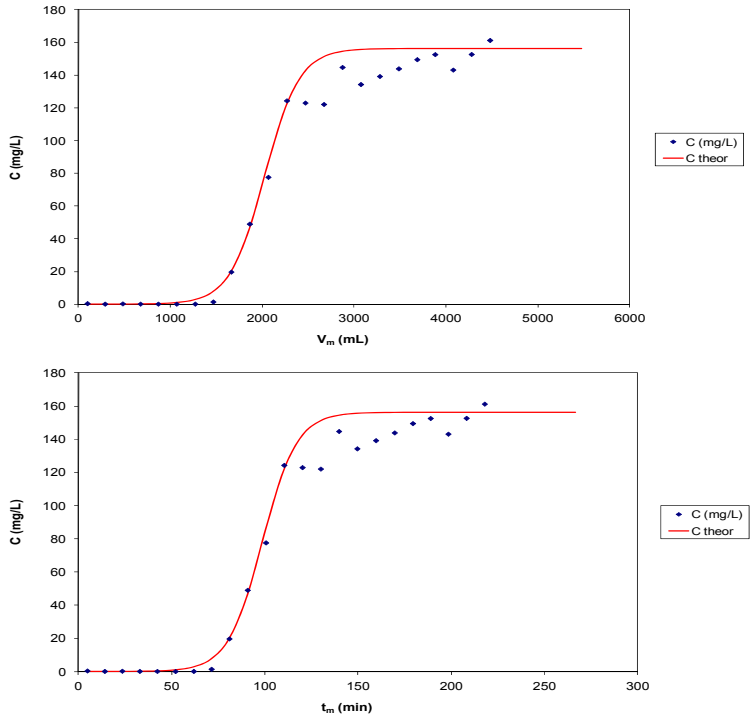

Fig. 3 Column experimental data and theoretical curves of MB adsorption on modified spruce; the effluent concentration is presented vs. (a) the effluent volume and (b) the adsorption time; x = 15 cm, C_i = 160 mg·L^{-1}, Q = 20 mL·min^{-1} (the theoretical curves are according to the Bohart and Adams model); modified by brine treatment; concentrated ×2 times at 160 °C for 10 min.

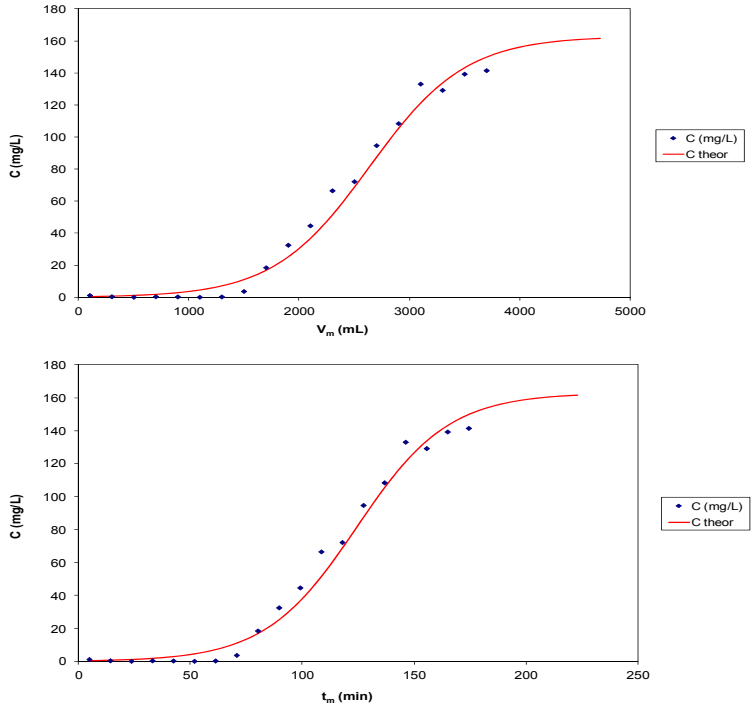

Fig. 4 Column experimental data and theoretical curves of MB adsorption on modified spruce; the effluent concentration is presented vs. (a) the effluent volume and (b) the adsorption time; x = 15 cm, C_i = 160 mg·L^{-1}, Q = 20 mL·min^{-1} (the theoretical curves are according to the Bohart and Adams model); modified by brine treatment; concentrated ×2 times at 160 °C for 50 min.

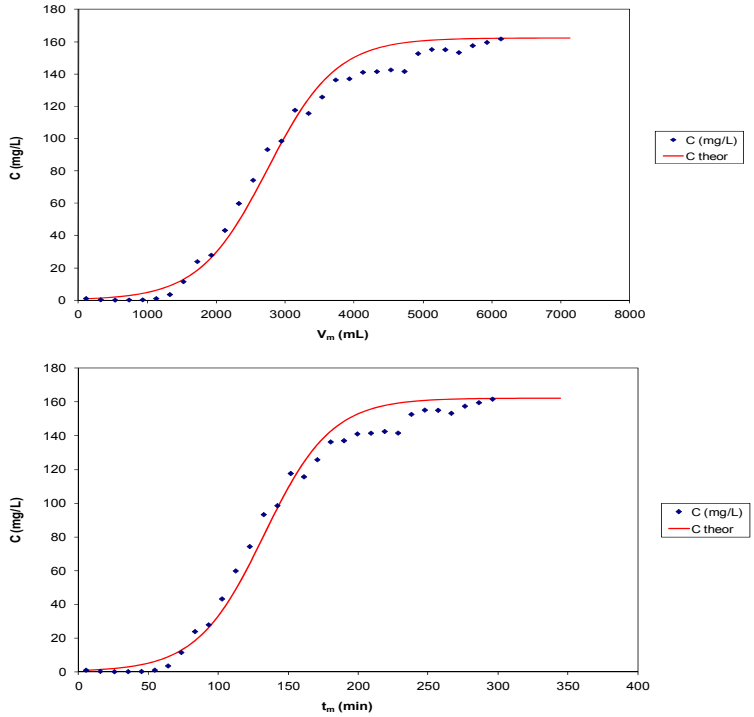

Fig. 5 Column experimental data and theoretical curves of MB adsorption on modified spruce; the effluent concentration is presented vs. (a) the effluent volume and (b) the adsorption time; x = 15 cm, C_i = 160 mg·L^{-1}, Q = 20 mL·min^{-1} (the theoretical curves are according to the Bohart and Adams model); modified by brine treatment; concentrated ×4 times at 180 °C for 0 min.

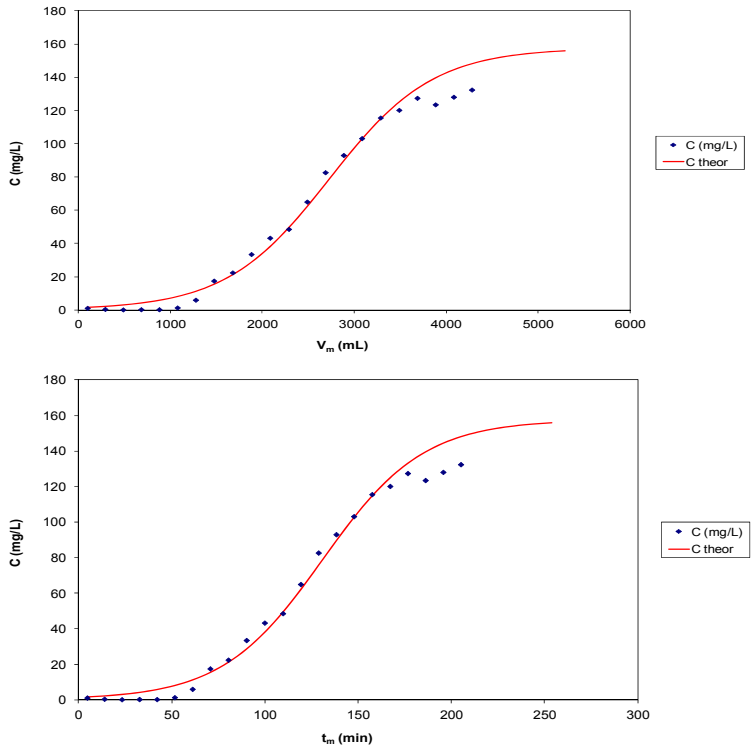

Fig. 6 Column experimental data and theoretical curves of MB adsorption on modified spruce; the effluent concentration is presented vs. (a) the effluent volume and (b) the adsorption time; x = 15 cm, C_i = 160 mg·L^{-1}, Q = 20 mL·min^{-1} (the theoretical curves are according to the Bohart and Adams model); modified by brine treatment; concentrated ×4 times at 200 °C for 50 min.

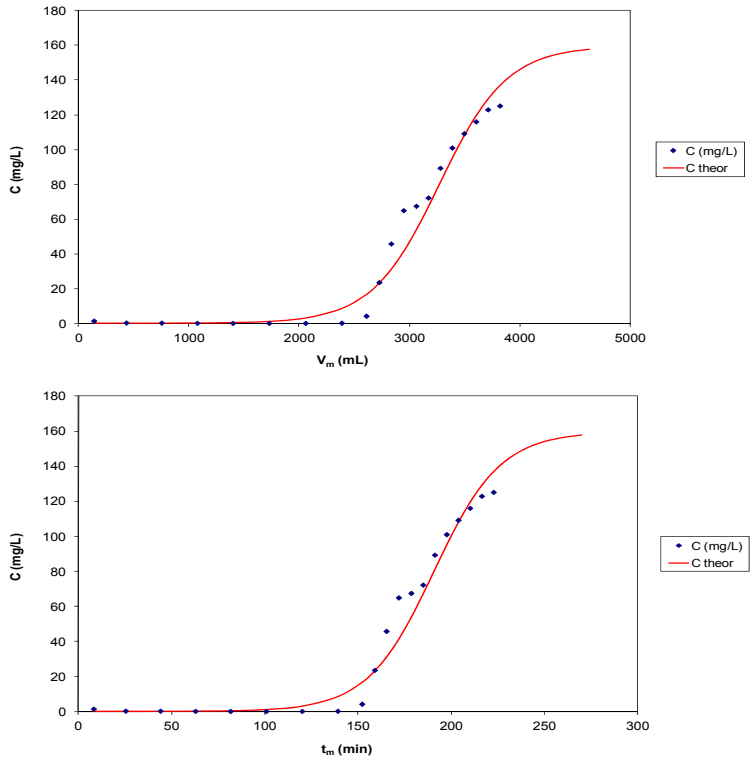

Fig. 7 Column experimental data and theoretical curves of MB adsorption on modified spruce; the effluent concentration is presented vs. (a) the effluent volume and (b) the adsorption time; x = 15 cm, C_i = 160 mg·L^{-1}, Q = 20 mL·min^{-1} (the theoretical curves are according to the Bohart and Adams model); modified by brine treatment; concentrated ×8 times at 180 °C for 50 min.

References

[1] Rafatullah, M., Sulaiman, O., Hashim, R., and Ahmad, A. 2010. "Adsorption of Methylene Blue on Low-Cost Adsorbents: A Review." *J. Hazard. Mater*. 177: 70-80.

[2] El-Sayed, A. M., Mitchell, V., Manning, L. A., Cole, L., and Suckling, D. M. 2011. "New Sex Pheromone Blend for the Lightbrown Apple Moth *Epiphyas postvittana*." *J. Chem. Ecol.* 37: 640-6.

[3] Altenor, S., Ncibi, M. C., Emmanuel, E., and Gaspard, S. 2012. "Textural Characteristics, Physiochemical Properties and Adsorption Efficiencies of Caribbean Alga *Turbinaria turbinata* and Its Derived Carbonaceous Materials for Water Treatment Application." *Biochem. Eng. J*. 67 (2): 35-44.

[4] Liu, T., Li, Y., Du, Q., Sun, J., Jiao, Y., Yang, G., et al. 2012. "Adsorption of Methylene Blue from Aqueous Solution by Grapheme." *Colloids and Surf. B: Biointerfaces*. 90: 197-203.

[5] Al-Anber, Z. A., Al-Anber, M. A., Matouq, M., Al-Ayed, O., and Omari, N. M. 2011. "Defatted Jojoba for the Removal of Methylene Blue from Aqueous Solution: Thermodynamic and Kinetic Studies." *Desalination* 276: 169-74.

[6] Malekbala, M., Hosseini, S., Yazdi, S. K., and Masoudi Soltani, S. 2012. "The Study of the Potential Capability of Sugar Beet Pulp on the Removal Efficiency of Two Cationic Dyes." *Chem. Eng. Res. Des.* 90: 704-12.

[7] Theydan, S. K., and Ahmed, M. J. 2012. "Adsorption of Methylene Blue onto Biomass-Based Activated Carbon by $FeCl_3$ Activation: Equilibrium, Kinetics, and Thermodynamic Studies." *J. Anal. Appl. Pyrol*. 97: 116-22.

[8] Ahmed, M. J., and Dhedanb, S. K. 2012. "Equilibrium Isotherms and Kinetics Modeling of Methylene Blue Adsorption on Agricultural Wastes-Based Activated Carbons." *Fluid Phase Equilibr.* 317: 9-14.

[9] Oliveira, W. E., Franca, A. S., Oliveira, L. S., and Rocha, S. D. 2008. "Untreated Coffee Husks as Biosorbents for the Removal of Heavy Metals from Aqueous Solutions." *J. Hazard. Mater*. 152: 1073-81.

[10] Reffas, A., Bernardet, V., David, B., Reinert, L., Bencheikh Lehocine, M., Dubois, M., et al. 2010. "Duclaux, Carbons Prepared from Coffee Grounds by H_3PO_4 Activation: Characterization and Adsorption of Methylene Blue and Nylosan Red N-2RBL." *J. Hazard. Mater*. 175: 779-88.

[11] Baek, M. H., Ijagbemi, C. O., Se-Jin, O., and Kim, D. S. 2010. "Removal of Malachite Green from Aqueous Solution Using Degreased Coffee Bean." *J. Hazard.*

Mater. 176: 820-8.

[12] Kyzas, G. Z., Lazaridis, N. K., and Mitropoulos, A. C. 2012. "Removal of Dyes from Aqueous Solutions with Untreated Biomass as Potential Low-Cost Adsorbents: Equilibrium, Reuse and Thermodynamic Approach." *Chem. Eng. J.* 189-190: 148-59.

[13] Freundlich, H. M. F. 1906. "Über die adsorption in lösungen, Zeitschrift für Physikalische." *Chemie.* 57: 385-471.

[14] Langmuir, I. 1916. "The Constitution and Fundamental Properties of Solids and Liquids." *J. Am. Chem. Soc*. 38: 2221-95.

[15] Sips, R. 1948. "Structure of a Catalyst Surface." *J. Chem. Phys*. 16: 490-5.

[16] Lagergren, S. 1898. "Zur theorie der sogenannten adsorption gelöster stoffe, Kungliga Svenska Vetenskapsakademiens." *Handlingar* 24: 1-39.

[17] Ho, Y. S., Ng, J. C. Y., and McKay, G. 2000. "Kinetics of Pollutants Sorption by Biosorbents: Review." *Sep. Purif. Methods* 29: 189-232.

[18] Weber, W. J., and Morris, J. C. 1963. "Kinetics of Adsorption on Carbon from Solution." *J. Sanit. Eng. Div. Am. Soc. Civ. Eng.* 89: 31-60.

[19] Bohart, G., and Adams, E. N. 1920. "Some Aspects of the Behavior of Charcoal with Respect to Chlorine." *J. Am. Chem. Soc.* 42: 523-44.

Journal of Environmental Science and Engineering B 7 (2018) 92-102
doi:10.17265/2162-5263/2018.03.002

Changing of Properties of Unsaturated Compacted Bentonite due to Hydration Effort

Tomoyoshi Nishimura[1] and Junichi Koseki[2]

1. Department of Civil Engineering, Ashikaga University, Ashikaga, Tochigi 326 8558, Japan

2. Department of Civil Engineering, The University of Tokyo, Bunkyo-ku, Tokyo 113 8654, Japan

Abstract: Radioactive waste disposal is important facility for human and environment in the world. Compacted bentonite in radioactive disposal engineer barrier design really experience hydration effort as decreasing of suction during long-time. Hydration effort develop macro-micro void structure in bentonite under deeply geological environment. The bentonite occurred uncertainly problems or translation in various experimental interaction boundary conditions such as thermal-hydration-chemical condition. To detect accumulation of deformation or changing of bentonite behaviour due to these processes is important that the modified experimental methods are required. In addition, to interpret laboratory experimental results combine to establish mathematical modelling in possible. The overall investigation or performance of the bentonite have contributed to represent the intrinsic properties of engineer barrier systems. This study focused on changing of properties of unsaturated compacted bentonite related to hydration effort due to increasing of relative humidity. Changing of some properties revealed to become instability or uncertainly problems in practice. Soil-water characteristic curve was measured with considering of various temperatures using vapor pressure technique. Swelling pressure and creep behaviour such as mechanical components were described with hydration effort.

Key words: Bentonite, suction, soil-water characteristic curve, swelling pressure, creep deformation.

1. Introduction

Radioactive waste disposals have been produced from atomic plant, and decommissioning of the nuclear power plants have supplied severe problems to environment. Deep geological disposal of radioactive waste or some of decommissioning of the nuclear power plants are science, technically and societally challenging duty. Geotechnical or Geo-environmental engineers in the world have approached some kind of mandate with the necessary honour and usefulness for highly generational protection of human. Actually, mount of radioactive disposal waste with some levels arises according to the nuclear energy legislation or as result of powerful economic activity. Unsaturated soil mechanics is required to response within the accurate framework for planning, construction, operating and maintenances of the considerable deep geological repositories. The safety design analyses for a deep geological repository was modified based on a comprehensive methods or measurement program of expansive materials such as bentonite, expansive clay and host rock. The general procedure has been evaluated by many laboratory tests and *in-situ* investigation [1-8].

The bentonite is one of interesting materials which consist of engineered barrier for deep geological repository. There are so many experimental reports in area of physical, science or technical. Following preliminary laboratory test, the work on swelling pressure test updated the enormous database or interpretations on the experiments that a number of synthesis reports were presented [9-16].

Working developments must advise the establish safety program to barrier system for submission of license application: one low and intermediate level waste and one for spent fuel, high-level and long lived intermediate-level waste. It is necessary to evaluation

Corresponding author: Tomoyoshi Nishimura, Professor, main research fields: unsaturated soil mechanics.

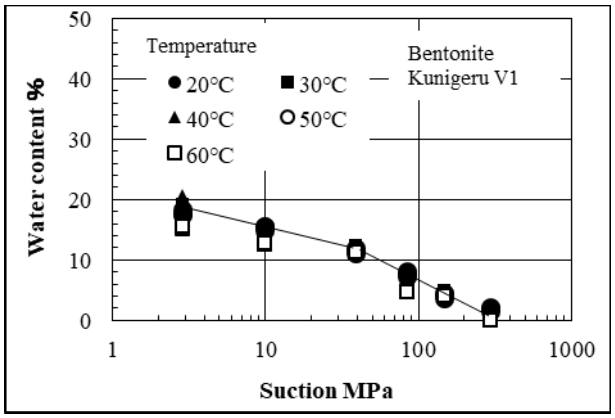

Fig. 1 SWCC with various temperatures.

of bentonite properties in unsaturated condition using suction control method or soil moisture retention concept [4, 17-27]. Many reports regard to soil-water characteristic curve or suction controlling procedure have been initiated to expand the mathematical simulation models [28-33]. Then, shear strength mechanics or experimental method with suction controlling supported the interpretation of unsaturated bentonite properties as scientific and technical background [34-46].

Recently, many data base obtained from geological field investigations in boreholes notice that there are uncertainly problems in the engineered barrier system such as hydration effort or thermal efforts. Hydration effort is one of factors associated to changing of relative humidity environment [47-53]. Thermal conductivity is one of parameters on Hydro-Thermal-Mechanical-Chemical simulations. Particularly, hydration effort induced the sever deformation to unsaturated bentonite. The deformation had closely creep behavior [54-61].

This study focused on hydration effort to properties of compacted bentonite, which was used as one component of radioactive disposal waste barrier system. Hydration induced volume deformation of compacted bentonite that changing of soil moisture cause, and vapour pressure technique was useful to control suction. Soil-water characteristic curve of compacted bentonite was indicated with both drying pass and wetting pass that increment of reduction in suction were applied to bentonite at term long-time. Also, swelling pressure was measured to compacted bentonite subjected to different suction. It was effort that suction decreased before swelling pressure test. All of these properties were measured using vapor pressure technique, which one of suction controlling methods. Also, the developed apparatus was used to appear creep behaviour of unsaturated compacted bentonite. After reduction of suction of bentonite, it was indicated that bentonite approached up to large deformation.

2. Soil-Water Characteristic Curve

2.1 Soil Material

The water retention activity is important feature which described as the soil-water characteristic curve (i.e. SWCC). The SWCC was one of key parameters for establishing of mathematical models, and basic physical parameter. Mechanical and hydration properties were evaluated using the SWCCs in the general soil material. The soil-water characteristic curves for sodium type bentonite were measured, which was Kunigel V1. SWCC test was conducted out using vapor pressure technique. The soil-water characteristic curve of sodium bentonite was indicated in Fig. 1. The specimens had no compaction that was powder condition. The determined SWCCs had a wide range from 2.8 MPa to 296 MPa which was obtained using the various salt solutions. Using vapor pressure technique for high suction measurement is no longer special suction application in unsaturated soil mechanics. In this testing, SWCCs was controlled with various temperature, which had a range from 20 degrees to 60 degrees, and difference was ten degrees. Obtained water contents in SWCC decreased with suction in drying process, and influence of temperatures on water content was quite small. It was possible to define one curve having an inflection point. So, unique opinion associated with increasing of temperature was not confirmed from these data sets.

The compacted unsaturated bentonite was prepared that changing of both water content and degree of saturation were measured under RH of 98%. RH 98% equilibrium with suction of 2.8 MPa, which was less than initial suction of compacted bentonite. Hydro effort imposed to bentonite, and soil moisture increased according to time. Phenomena-induced hydration were shown in Figs. 2 and 3. Increment of water content was obtained to measure changing of weight of specimen with time, and degree of saturation was calculated using changing of weight and changing of both diameter and height at any time.

The compacted bentonite had a dry density of 1.600 g/cm^3 before applying of hydration. Increment of both water content and degree of saturation proved to induce the deformation of bentonite by increasing soil moisture due to hydration effort.

It is important to investigate the influence of salt solution on water retention activity of compacted bentonite. This study conducted out SWCC test for saturated bentonite in salt water. Saturated bentonites were prepared for measurement of SWCC that one was swelled in the distilled water, and another one was swelled in the salt water (i.e. NaCl water). Salt water had 3.5% in concentration, which was similar to nature sea water. Each bentonite was dry density of 1.600 g/cm^3 at initial condition and had no mixture sand. Compacted bentonite with water content of 8.0% was absorbed in each bentonite was dry density of 1.600 g/cm^3 at initial condition and had no mixture sand. Compacted bentonite with water content of 8.0% was absorbed in steel mould, and initial specimen size was a height of 2.0 cm and a diameter of 6.0 cm, respectively. Absorbing a bentonite specimen was conducted under constant initial volume during over one month. After swelling, it was confirmed that each specimen approached to saturation in the steel mould. Each saturated bentonite was placed into glass desiccator with salt solutions. Variety salt solutions produced specified relative humidity that was vapor pressure technique. This testing program used seven different salt solutions, and controlled relative humidity had a range from 98% to 11%. Using relative humidity ranges corresponded that suction had a rage from 2.8 MPa to 286 MPa.

As first testing step, saturated bentonite was placed into RH 98% environment in glass desiccator, and this step maintained over one month. On evaluation of equilibrium with relative humidity to bentonite specimen, a period of one month was in generally accepted in SWCC test procedures, was recognized as one of practice methods in conventional. When specimen took an equilibrium, some parameters were measured which were weight, diameter and height for specimen, and determine water content and degree of saturation to controlled suction. Step by step, suction was decreased up to 286 MPa due to replace salt solutions in drying process. Relative humidity in glass desiccator according to be reduction that relative humidity was 11% at end of drying process. All of

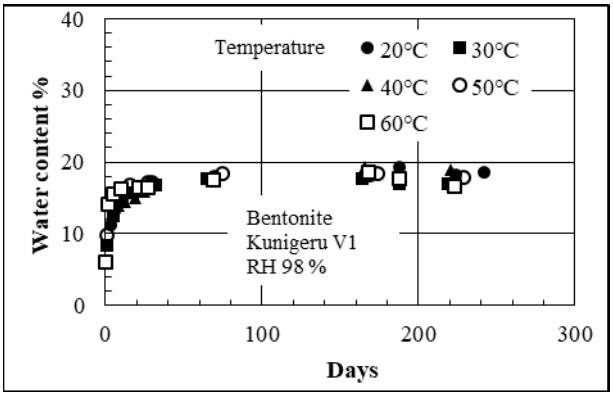

Fig. 2 Increment of water content according to hydration.

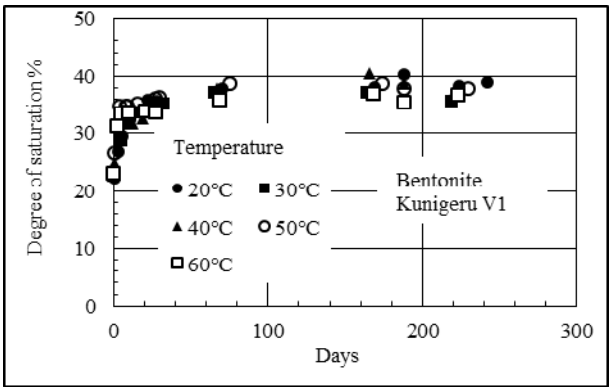

Fig. 3 Increment of degree of saturation under according to hydration.

suctions were seven different values in drying process.

Subsequently, wetting process-induced by reduction of suction was commencement to all bentonite specimens experienced drying process. Suctions on process in wetting procedure were quite same that it was easy to comparison to observing test results at drying process. Above mentioned, physical properties such as water content and degree of saturation were determined with same testing methods.

Both water content and degree of saturation such as parameters were used to describe each SWCC of bentonite (Fig .2 from 4 to 7). On drying process, soil moisture was obviously large for bentonite including salt component up to suction of 9.8 MPa. Beyond suction was 9.8 MPa, reduction of water content with increment of suction was indicated, and thus results were similar between bentonites with and without salt water at drying process. Also, water contents were

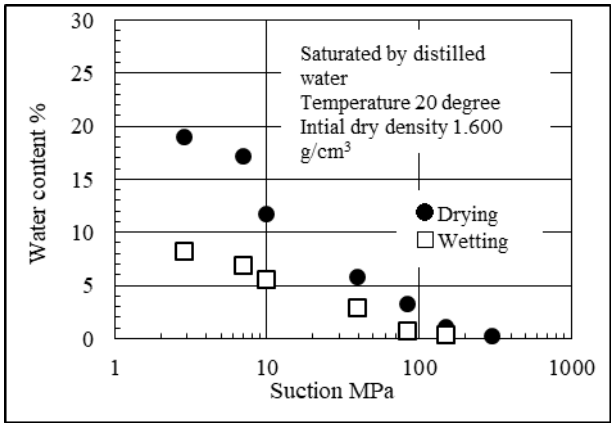

Fig. 4 Changing of water content (distilled water).

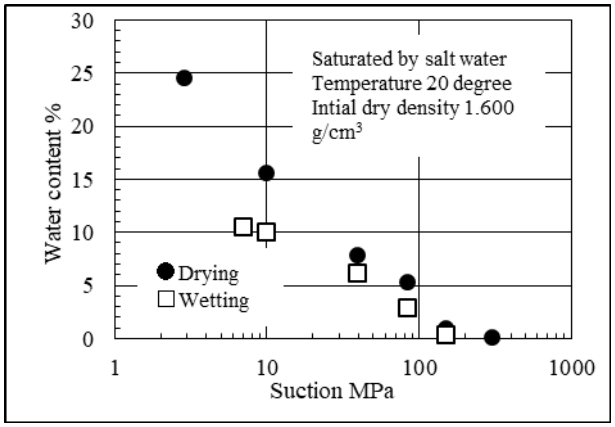

Fig. 5 Changing of water content (salt water).

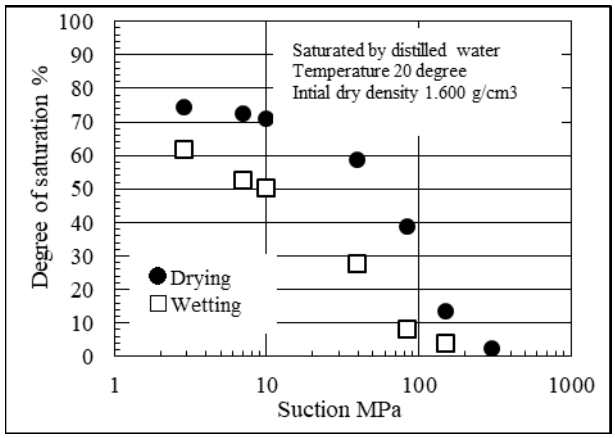

Fig. 6 Changing of degree of saturation (distilled water).

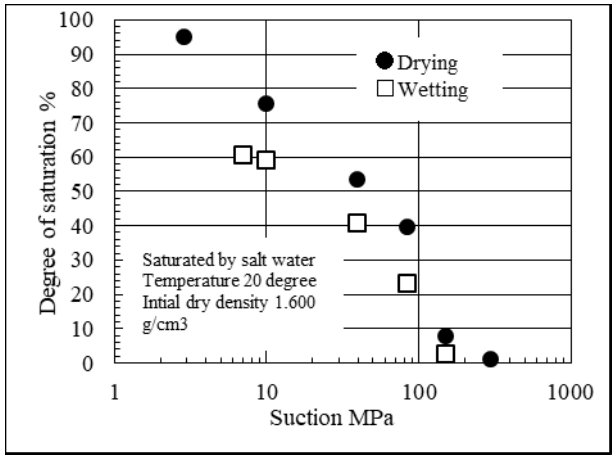

Fig. 7 Changing of degree of saturation (salt water).

measured near zero value regardless of imposing salt components at suction of 296 MPa.

On wetting process, all bentonite specimens described to increase soil moisture regardless of experience with and without salt water that it was widely accepted in water retention mechanics in unsaturated soils. Water content and degrees of saturation can seem to be not same with those data sets of bentonites in drying process that exist much hysteresis in hydro-processing. Particularly, the bentonite with salt component indicated large increment of soil moisture with reduction of suction comparison with observing results in de-stilled water. As results, few hysteresis was observed in the bentonite having salt components that strong efforts contributed to water retention activity associated with bentonite properties.

3. Swelling Pressure of Unsaturated Bentonite Subjected to RH

Swelling pressure is one of important key parameters for construction of radioactive waste disposal system which is supplied saturation process under deep ground during long term period. Many reports regard to swelling properties of variety bentonites had been established that almost of swelling tests were conducted to supply water absorbing to unsaturated bentonite directly. It is sure that barrier structure constructed using unsaturated bentonite was initially unsaturated condition, and considerable slow water flow is predicted as results of many mathematical simulation models. To reach to completely saturation situation spend extremely long times. While unsaturated bentonite become toward to saturation, hydration effort make slowly expansion in changing of suction of bentonite under deep tunnel. It was no consider that deformation of unsaturated bentonite occurs according to suction reduction (i.e. increment of relative humidity).

A swelling pressure testing apparatus was developed to determine swelling pressure in a constant relative humidity environment. The apparatus consists of a triaxial chamber and relative humidity control circulation system. The modified swelling pressure testing apparatus was shown in Fig. 8 that consisted mainly of a triaxial chamber, a pedestal, a steel mold, a double glass burette, a differential pressure transducer, a difference displacement sensor, load cell sensor and relative humidity control circulation system. The relative humidity control circulation system was established using a conventional pump, along with a small chamber with salt solution. The air flow maintained a constant relative humidity surrounding the compacted bentonite. All compacted bentonite specimens were placed into steel mould. Moving water in the double glass burette due to absorption in bentonite was permitted at the low portion of specimen. Absorption water volume change in the double burette was measured using the differential pressure transducer. Initial total volume was maintained constant for all compacted bentonite specimens.

Sodium bentonite was used for measurement of swelling pressure. Silica sand had uniformity grain size distribution which was mixed with bentonite at a ratio of 30% by dry weight. The specimen was statically compacted in stiffness steel mold at an initial water content of 5.9%. The compacted bentonite

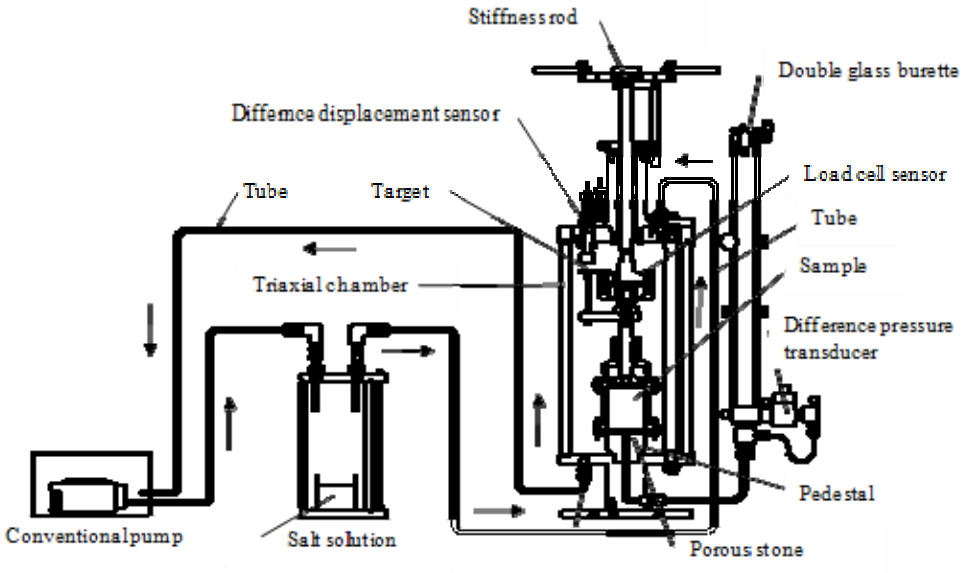

Fig. 8 Modified swelling pressure test apparatus.

specimen had a dry density of 1.600 g/cm^3 as target value. The height of specimen was 25.5 mm. Compacted bentonite specimens with two different soil suctions were prepared for swelling pressure tests.

Initial compacted bentonite had a soil suction of 105 MPa. Soil suction of 2.8 MPa was imposed using vapor pressure technique and used salt solution was Potassium Sulfate.

Soil suction of 2.8 MPa corresponds to relative humidity of 98%. The gravimetric water content increased that vapour moisture in RH 98 was absorbed into void structure of bentonite having suction of 105 MPa. As result, the gravimetric water content of the compacted bentonite sample subjected to relative humidity of 98% increased to 9.7% from 5.9%. Also, deformation in expansion occurred, grew with time. Finally, deformation of bentonite specimen took large expansion in vertical direction, and was 9.5% in swelling. During hydration process, void structure constructed macro-micro structure produce complexly expansion in clay structures together. Changing of total volume was useful to determine dry density. The dry density of the sample after equilibrium soil suction of 2.8 MPa decreased to 1.427 g/cm^3 from 1.600 g/cm^3.

Swelling pressure of bentonite with two different suctions were measured under constant volume, which changing of a height of specimen was not permitted through swelling test.

Fig. 9 shows observing the swelling pressures with water absorb for compacted bentonite at initial water content of 5.9%, and specimen had an initial soil suction of 105 MPa at beginning test. The measured swelling pressure described rapidly growing during almost 50 hours periods. Strong increment of swelling pressure seems to be one of characters on swelling properties for compacted bentonite with high suction. Determined swelling pressure at 50 hours was 220 kPa. Behind 220 kPa in swelling pressure, bentonite described traditionally small reduction with time. Reduction continued smoothly till elapsed time was 350 h, and measured swelling pressures had date sets with both increment and decrement such as a frequency cyclic motion. Once again, the bentonite showed small increment, which appeared increment and decrement in swelling pressure. Its smoothly increasing was maintained till swelled bentonite took equilibrium, and elapsed time was nearly 1,000 hours. Confirmed maximum swelling pressure corrected as 267 kPa.

The compacted bentonite with soil suction of 2.8 MPa shows smoothly increasing of swelling pressure at beginning of test as shown in Fig. 10. There was quite difference comparison to swelling behaviour of initial suction of 105 MPa. It was obviously that

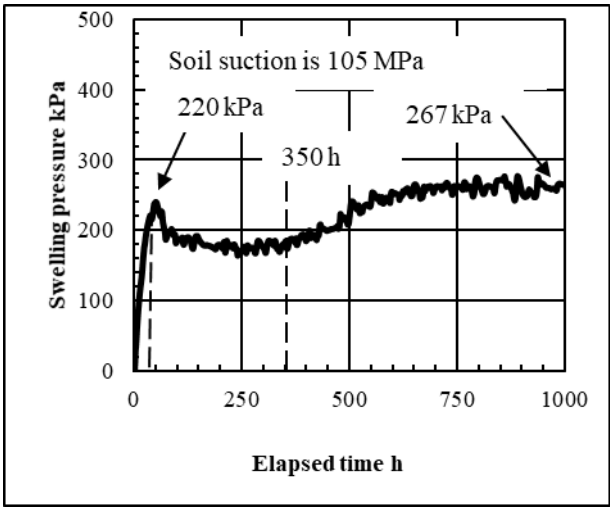

Fig. 9 Processing of swelling pressure (no hydration).

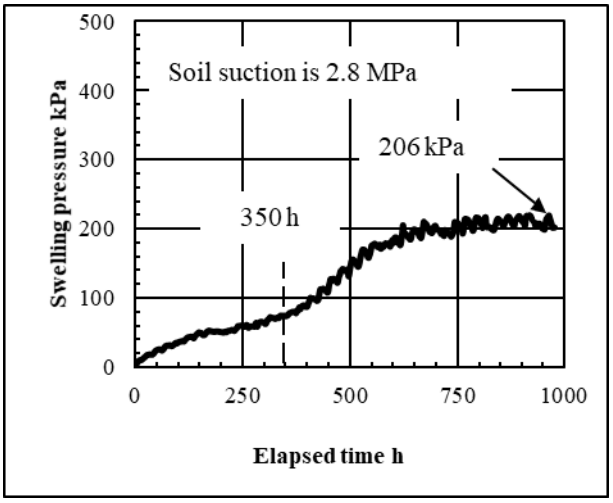

Fig. 10 Processing of swelling pressure (hydration).

performed swelling pressure was smaller than that of suction 105 MPa at beginning that was revealed as the influence of suction of bentonite before absorbing. Growing of swelling pressure was extremely slow till elapsed time was 350 h that was entirely difference against to swelling pressure increment mentioned in Fig. 9.

After the elapsed time of 350 hours, accumulation of swelling performance became to be developed, and it reached to 200 kPa at 650 hours. Beyond 750 hours, bentonite seemed to be equilibrium that 206 kPa was measured as maximum swelling pressure. Bentonite showed that hydration effort caused reduction of swelling pressure, and at same time growing processes of swelling pressure was quite difference between with and without hydration effort before swelling process. Consequently, degree of saturation obtained from water content at end of test reached to saturation regardless of magnitude of suction value before swelling.

4. Creep Test

This study mad above mention that hydration effort such as reduction of suction improved both water retention capacity and swelling performance in compacted bentonite. Revised basic properties to compacted bentonite was induced at macro-micro structure as extremely fine structures. This testing conducted out creep test and finding relationship between main chief factor in hydration effort and strength resistance in mechanical properties. It is defined in generally for the soil mechanics that creep test is conducted under constant effective stress to saturated soils. The changing of macro-micro void structure due to hydration effort had closely the deformation on creep behavior. The modified creep test apparatus was shown in Fig. 11. The apparatus employed a conventional cyclic relative humidity control system, which was possible to apply a required RH using vapor pressure technique. This apparatus consists of triaxial chamber, air cyclic flow pump. A dynamic activity of the conventional pump had at least 10 kPa pressure, which maintained steady air flow through the system.

Creep stresses were determined using unconfined compressive strength in experimental data sets what was deviator stress without confining pressure. Controlled relative humidity was either 98%. In case of RH 98%, suction of 2.8 MPa corresponding to RH 98% was considerable lows level suction comparison with suction of bentonite in initial condition. Used specimen had both a height of 100 mm and a diameter of 50 mm, respectively. Also, dry density was 1.600 g/cm^3 as target value.

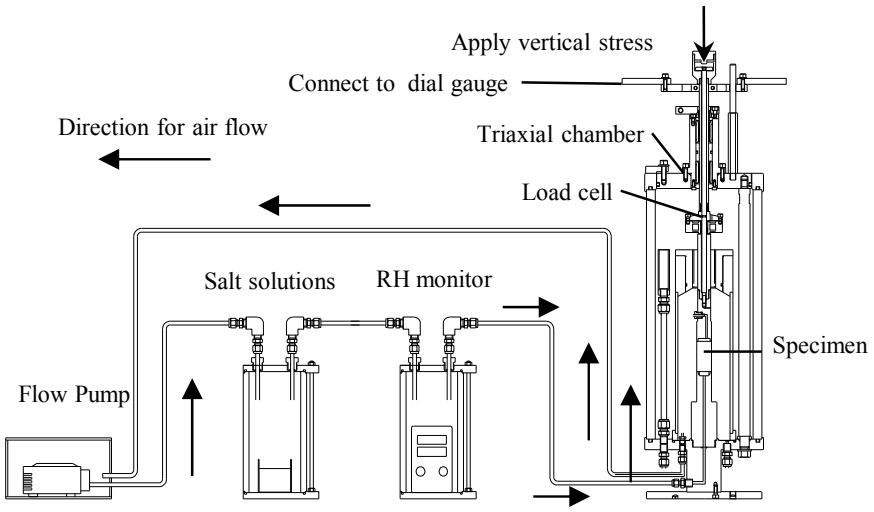

Fig. 11 Modified creep test apparatus.

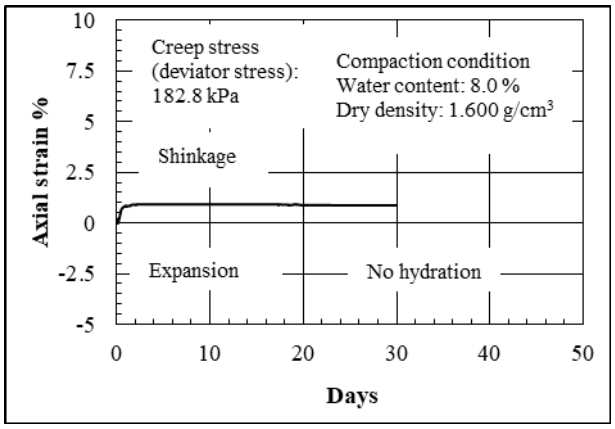

Fig. 12 Case of no hydration for creep test.

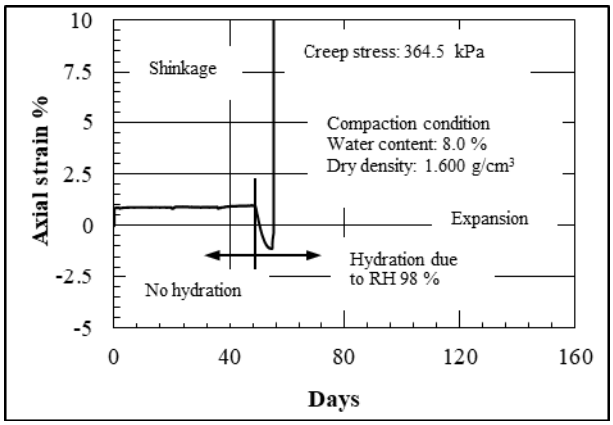

Fig. 13 Case of application of hydration for creep test.

Observing axial strain under subjection of external vertical loading was shown in Fig. 12. Prepared creep stress was 182.8 kPa and was maintained till end of test. Then, positive value in axial strain expressed that specimen occurred compression deformation. The axial strain in shrinkage was approximately 1.0% at beginning of external loading, which was produced by deviator stress as mechanical action. The axial strain was remained a period of 30 days (i.e. up to end of test). It was able to predicate that the specimen described growing shrinkage deformation under no hydration environment.

As other case, axial strains with elapsed time was indicated as shown in Fig. 13, and applied creep stress was 364.5 kPa more than that mentioned in Fig. 12. Though bentonite had creep stress of 364.5 kPa under no hydration till fifty days, compression deformations were measured at commencement of supplying vertical load. While fifty days, axial strain described a stable, and the strains were similar with measured strain on beginning of loading of stress. There were not observing increment of shrinkage strain such as creep deformation.

Subsequently, the hydration was applied to bentonite due to air flow having RH 98%, and suction surrounding of specimen approached rapidly 2.8 MPa in suction. As point of view regard to presence or absence in hydration effort, beyond fifty days the bentonite occurred the expansion distinctly with days. It was sure that the effort of hydration was revealed with measured changing of vertical strain. The processing of hydration effort developed macro-micro structures in bentonite, and large increment of expansion was described from forty days to fifty days. At fifty days, specimen had large expansion comparison with initial height that measured expansion strain was approximately 1.0%. Subsequently, the bentonite evidenced the shrinkage deformation such as up to destruction. Thus, axial strain data sets indicated straight line in vertical direction. Crushed specimen was clearly observed in chamber. Then, the hydration effort can be defined as decrement of suction in stress variables that induced the destruction combined large deformations for unsaturated bentonite.

5. Conclusions

This study represented properties of bentonite such as extremely expansive soils on experimental resulting. The hydration effort to compacted bentonite was referred as one of significant impact factors, which induced uncertainly conditions on engineered properties to unsaturated bentonite. On supporting unsaturated soil mechanics, some experimental laboratory tests were conducted used modified apparatus that were SWCC test, swelling pressure test and creep test for unsaturated compacted bentonite. These tests had enough advantage to investigation above mentioned physical and mechanical properties

of compacted bentonite. Particularly, interpretation incorporated suction controlling methods were useful to understand the influence of hydration effort such as reduction suction on bentonite properties:

(1) The bentonite had high water retention activity at high suction ranges such as larger than 2.8 MPa in suction. The hydration effort induced expansion of the volume under reduction of suction, and, increment of soil moisture occurred at same time. Also, reduction of suction was controlled using vapor pressure technique that relative humidity was directly controlled in mythology.

(2) The obtained soil-water characteristic curves of bentonite can affirm that the influence of temperature on water retention activity was negligible. Other hands, the salt water produced to be high soil retention activity that bentonite absorbed, swelled in the salt water.

(3) Due to suction reduction, the swelling pressure with time indicated smoothly growing comparison to initial condition (i.e. before applying of hydration). As results, peak swelling pressure decreased that the transmutation of macro-micro void structure in bentonite immediately related to performance of swelling behavior.

(4) Through creep test, when hydration effort such as suction reduction was applied to compacted bentonite, it was obviously that axial strain in expansion direction was observed, and unsaturated compacted bentonite reached up to failure as result of maintain of both hydration effort and creep stress loading.

References

[1] Buscher, F., and Muller-Vonmoos, M. 1989. "Bentonite as a Containment Barrier for the Disposal of Highly Radioactive Waste." *Applied Clay Science* 4 (2): 157-177.

[2] Cui, Yu-Jun., and Anh, Minh, Tang. 2013. "On the Chemo-thermo-hydro-mechanical Behavior of Geological and Engineered Barriers." *Journal of Rock Mechanics and Geotechnical Engineering* 5 (3): 169-178.

[3] Gens, A., Vallejian, B., Zandrain, M. T., and Sanchez, M. 2013. "Homogenization in Clay Barrier and Seals: Two Case Studies." *Journal of Rock Mechanics and Geotechnical Engineering* 5: 191-199.

[4] Hoffman, C., Romero, E., and Alonso, E. E. 2005. "Combing Different Controlled-suction Technique to Study expansive Clays." *Proceedings of an International Symposium on Advanced Experimental Unsaturated Soil Mechanics EXPERUS* 2005: 61-67.

[5] Munoz, J. J., Alonso, E. E., and Lloret, A. 2009. "Thermo-hydraulic Characterization of Soft Rock by Means of Heating Stress." *Geotechnique* 59 (4): 293-306.

[6] Push, R. 1982. "Mineral-water Interactions and Their Influence on the Physical Behavior of Highly Compacted Na-Bentonite." *Canadian Geotechnical Journal* 19: 381-387.

[7] Sanchez, M., Gen, A., and Guimaraes, L. 2012. "Thermal-hydraulic-mechanical (THM) Behaviour of Large-scale in situ Heating Experiment during Cooling and Dismantling." *Canadian Geotechnical Journal* 49 (10): 1169-1195.

[8] Shackelford, C. D. 1991. "Laboratory Diffusion Testing for Waste Disposal." *Journal of Contaminant Hydrology* 7: 177-217.

[9] Chu, T. Y., and Mou, C. H. 1973. "Volume Change Characteristics of Expansive Soils Determined by Controlled Suction Tests." *Proceedings of the Third International Conference on Expansive Soils* 1: 177-185.

[10] Dakshinamurthy, V. 1978. "A New Method to Predict Swelling using Hyperbolic Equation." *Geotechnical Engineering* 9 (1): 1978: 29-38.

[11] Kodandaramaswamy, K., and Rao, S. N. 1981. "The Prediction of Settlements and Heave in Clays." *Canadian Geotechnical Journal* 17 (4): 623-631.

[12] Komine, H., and Ogata, N. 1999. "Experimental Study on Swelling Characteristics of Sand-bentonite Mixture for Nuclear Waste Disposal." *Soils and Foundations* 39 (2): 83-97.

[13] Nishimura, T., Koseki, J., and Matsumoto, M. 2012. "Measurement of Swelling Pressure for Bentonite under Relative Humidity Control." *Unsaturated Soils Research and Applications E-UNSAT* 1: 235-240.

[14] Push, R., and Yong, R. 2003. "Water Saturation and Retention of Hydrophilic Clay buffer Micro-structural Aspects." *Applied Clay Science* 23: 61-68.

[15] Sridharan, A., and Jayadeva, M. S. 1982. "Double Layer Theory and Compressibility of Clays." *Geotechnique* 32 (2): 133-144.

[16] Sridharan, A., Rao, A. S., and Sivapullaiah, P. V. 1986. "Swelling Pressure of Clays." *Geotechnical Testing Journal, ASTM* 9 (1): 24-33.

[17] Alonso, E. E., Romero, E., and Hoffmann, C. 2205. "Expansive Bentonite–sand Mixtures in Cyclic

Controlled-suction Drying and Wetting." *Engineering Geology* 81: 213 226.

[18] Barbour, S. L., and Fredlund, D. G. 1989."Mechanisms of Osmotic Flow and Volume Change in Clay Soils." *Canadian Geotechnical Journal* 26: 551-562.

[19] Barbour, S. L. 1998. "Nineteenth Canadian Geotechnical Colloquium: The Soil-water Characteristic Curve: a Historical Perspective." *Canadian Geotechnical Journal* 35: 873-894.

[20] Blatz, J. A., and Graham, J. and Chandler, N. A. 2002. "Influence of Suction on the Strength and Stiffness of Compacted Aand-bentonite." *Canadian Geotechnical Journal* 39: 1005-1015.

[21] Delage, P., Romero, E. E., and Tarantino, A. 2008. "Recent Developments in the Techniques of Controlling and Measuring Suction in Unsaturated Soils." *Proceedings of the First European Conference on Unsaturated Soils E-UNSAT*, 2008: 33-52.

[22] Kassiff, G., and Shalom, A. B. 1971. "Experimental Relationship between Swell Pressure and Suction." *Geotechnique* 21 (2): 245-255.

[23] Lagerwerff, J. V., Ogata, G., and Eagle, H. E. 1961. "Control of Osmotic Pressure of Culture Solutions with Polyethylene Glycol." *Science* 133: 1486-1487.

[24] Leong, E. C., and Rahardjo, H. 1997. "Review of Soil-water Characteristic Curve Equations." *Journal of Geotechnical and Geoenvironmental Engineering* 123 (12): 1106-1117.

[25] Oteo-Mazo, C., Saez-Aunon, J., and Esteban, F. 1995. "Laboratory Tests and Equipment with Suction Ccontrol." *Proceedings of the 1st International Conference on Unsaturated Soils*, Paris 3: 1509-1515.

[26] Romero, E. 2001. "Controlled Suction Techniques." *4th Simposio Brastileiro de Solos Nao Saturados* 2001: 535-542.

[27] Romero, E,. Vaunat, J., and Merchan, V. 2014. "Suction Effects on the Residual Shear Strength of Clays." *Journal of Geo-Engineering Science* 2: 17-37.

[28] Alonso, E. E., Gens, A., and Josa, A. 1990. "A Constitutive Model for Partially Saturated Soils." *Geotechnique* 40 (3): 405- 430.

[29] Alonso, E. E., Vaunat, J., and Gens, A. 1999. "Modelling the Mechanical Behavior of Expansive Clays." *Engineering Geology* 54: 173-183.

[30] Alonso, E. E., Pereira, J. M., Vaunat, J., and Olivella, S. A. 2010. "Microstructurally based Effective Stress for Unsaturated Soils." *Geotechnique* 60 (12): 913-925.

[31] Alonso, E. E., Zandarin, M. T., and Olivella, S. 2013. "Joints in Unsaturated Rocks: Thermo-hydro-mechanical Formulation and Constitutive Behaviour." *Journal of Rock Mechanics and Geotechnical Engineering* 5 (3): 200-213.

[32] Blatz, J. A., and Graham, J. 2003. "Elastic-plastic Modelling of Unsaturated Soil using Results from a New Triaxial Test with Controlled Suction." *Geotechnique* 53 (1): 113-122.

[33] Gens, A., and Alonso, E. E. 1992. "A Framework for the Behaviour of Unsaturated Expansive Clays." *Canadian Geotechnical Journal* 29: 1013-1032.

[34] Boso, M., Tarantino, A., and Mongiovi, L. 2005. "A Direct Shear Box Improved with the Osmotic Technique." *Proceedings of an International Symposium on Advanced Experimental Unsaturated Soil Mechanics EXPERUS* 2005: 85-91.

[35] Chavez, C., Romero, E., and Alonso, E. E. 2009. "A Rockfill Triaxial Cell with Suction Control." *Geotechnical Testing Journal* 32 (3): 1-13.

[36] Escario, V. 1980. "Suction Controlled Penetration and Shear Tests." *Proceedings of the Fourth International Conference on Expansive Soils* 2: 781-797.

[37] Escario, V., and Saez, J. 1986. "The Shear Strength of Partly Saturated Soils." *Geotechnique* 36 (3): 453-456.

[38] Fredlund, D. G. 1987. "The Stress State for Expansive Soils." *Proceedings of Sixth International Conference on Expansive Soils,* New Delhi India: 1-9.

[39] Likos, W. J., Wayllace, A., Godt, J., and Lu, N. 2010. "Modified Direct Shear Apparatus for Unsaturated Sands at Low Suction and Stress." *Geotechnical Testing Journal* 33 (4): 286-298.

[40] Nishimura, T., Hirabayashi, Y., Fredlund, D. G., and Gan, J. K-M. 1999. "Influence of Stress History on the Strength Parameters of an Unsaturated Statically Compacted Soil." *Canadian Geotechnical Journal* 36: 251-261.

[41] Nishimura, T., Fredlund, D. G. 2001. "Failure Envelope of a Desiccated, Unsaturated Silty Soil." *Proceedings of the 15th International Conference on Soil Mechanics and Geotechnical Engineering*, Istanbul, 1: 615-618.

[42] Nishimura, T., and Fredlund, D. G. 2003. "A New Triaxial Apparatus for High Total Suction using Relative Humidity Control." *12th Asian Regional Conference on Soil Mechanics and Geotechnical Engineering*: 65-68.

[43] Nishimura, T., and Vanapalli, S. K. 2005. "Volume Change and Shear Strength Behavior of an Unsaturated Soil with High Soil Suction." *16th International Conference on Soil Mechanics and Geotechnical Engineering*: 563-566.

[44] Nishimura, T., Rahardjo, H., and Koseki, J. 2010. "Direct Shear Strength of Compacted Bentonite under Different Suctions." *Proceedings of The Fifth International Conference on Unsaturated Soils Barcelona Spain*: 323-328.

[45] Nishimura, T. 2011. "Influence of Decreasing of Soil Suction on Unconfined Compressive Strength for

Bentonite." *Proceedings of First International Conference GeoMat* 2011 1: 103-106.

[46] Nishimura, T., and Koseki, J. 2011. "Effect of Suction on Direct Shear Strength of Compacted Bentonite." *Proceedings of The 14th Asian Regional Conference on Soil Mechanics and Geotechnical Engineering*: 203-208.

[47] Alonso, E. E., and Pineda, J. A. 2007. "Degradation of Argillaceous Rocks: A Challenge for Unsaturated Geomechanics." *Proceedings of the 3rd Asian Conference on Unsaturated Soils*: 3-26.

[48] Botts, M. E. 1998. "Effects of Slaking on the Strength of Clay Shales." In Evangelista and Picarelli (eds.), *The Geotechnics of Hard Soils-Soft Rocks Rotterdam*: 447-458.

[49] Fredlund, D. G., and Rahardjo, H. 1993. "Chapter 4, Measurement of Soil Suction." Soil Mechanics for Unsaturated Soils A Wiley-Interscience Publication JOHN WILEY & SONS INC: 64-106.

[50] Marinho, F. A. M., Take, W. A., and Tarantino, A. 2008. "Measurement of Matric Suction using Tensiometertic and Axis Translation Techniques." *Geotechnical and Geological Engineering* 26: 615-631.

[51] Morodome, S., and Kawamura, K. 2009. "Swelling Behavior of Na- and Ca-montmorillonite up to 150 °C by In situ X-ray Diffraction Experiments." *Clays and Clay Minerals* 57 (2): 150-160.

[52] Peng, X., and Horn, R. 2007. "Anisotropic Shrinkage and Swelling of Some Organic and Inorganic Soils." *European Journal of Soil Science* 58 (1): 98-107.

[53] Romero, E., Alonso, E., Alvarado, C., and Wacker, F. "Effect of Loading History on Time Dependent Deformation of Rockfill." *Unsaturated Soils Research and Applications E-UNSAT 2012*, 1: 419-424.

[54] Duttine, A., Tatsuoka, F., Salotti, A., and Ezaoui, A. 2015. "Creep and Stress Relaxation Envelopes of Granular Materials in Direct Shear." *Proc. of 6th International Conference on Deformation Characteristics of Geomaterials Buenos Aires*: 494-502.

[55] Ezaoui, A., Tatsuoka, F., Duttine, A., and Di Benedetto, H. 2011. "Creep Failure of Geomaterials and Its Numerical Dimulation." *Geotechnique Letter*: 1-5.

[56] Kawabe, S., and Tatsuoka, F. 2015. "1D Creep and Delayed Rebound during Unloading and Reloading of Clay and Its Model Simulation." *Deformation Characteristics of Geomaterials Proc. of 6th International Conference on Deformation Characteristics of Geomaterials Buenos Aires*: 486-493.

[57] Kongkitkul, W., Tatsuoka, F., and Hirakawa, D. 2007. "Creep Rupture Curve for Simultaneous Creep Deformation and Degradation of Geosynthetic Reinforcement." *Geosynthetics International* 14 (4): 1-12.

[58] Lloret, A., Villar, M. V., Sanchez, M., Gens, A., Pintado, X., and Alonso, E. E. 2003. "Mechanical Behavior of Heavily Compacted Bentonite under High Suction Changes." *Geotechnique* 53 (1): 27-40.

[59] Tatsuoka, F., Uchimura, T., Tateyama, M., and Muramoto, K. 1996. "Creep Deformation and Stress Relaxation in Preloaded/Prestressed Geosynthetic-reinforced Soil Retaining Walls Measuring and Modelling-Time-Dependent Soil Behavior." *Geotechnical Special Publication ASCE Washington Convention*: 258-272.

[60] Tatsuoka, F., Di Benedetto, H., and Nishi, T. 2003. "A Framework for Modelling of the Time Effects on the Stress-strain Behaviour of Geomaterials." *Proc. 3rd Int. Sym. on Deformation Characteristics of Geomaterials IS Lyon 03 (di Benedetto et al. eds.) Balkema*: 1135-1143.

[61] Tatsuoka, F., Duttine, A., Salotti, A., and Ezaoui, A. 2015. "Creep and Stress Relaxation of Granular Materials Simulated by Non-linear Three Component Model." Deformation Characteristics of Geomaterials, *Proc. of 6th International Conference on Deformation Characteristics of Geomaterials, Buenos Aires*: 503-510.

Journal of Environmental Science and Engineering B 7 (2018) 103-110
doi:10.17265/2162-5263/2018.03.003

Stepwise Regression: An Application in Earthquakes Localization

Giuseppe Pucciarelli
Dept. of Physics "E. R. Caianiello", University of Salerno, Fisciano 84084, Italy

Abstract: In this paper, an overview of an important feature in statistics field has shown: the stepwise multiple linear regression. Likewise, a link between stepwise multiple linear regression and earthquakes localization has been descripted. Precisely, the aim of this research is showing how stepwise multiple linear regression contributes to solution of earthquakes localization, describing its conditions of use in HYPO71PC, a software devoted to computation of seismic sources' collocation. This aim is reached treating a concrete case, that is computation of earthquakes localization happening on Mount Vesuvius, Italy.

Key words: Stepwise regression, earthquakes localization, Geiger's method, HYPO71PC, Mount Vesuvius.

1. Introduction

Linear regression is probably the simplest and, at same time, the most well-known method of research of a mathematical relation between an explanatory variable and a dependent one of physical quantities. A particular specification is about the case in which explanatory variables are more than ones, that is the case of multiple linear regression. Basic concept is to establish a priori that physical quantities which are at stake are linked with each other in a linear way by means of a mathematical relation, named linear model. The goal is finding the parameters of this model, starting from observed data. A particular type of these statistical models is the so-called SMLR (Stepwise Multiple Linear Regression). In this regression typology, computation of model's parameters happens by means of an algorithm. In this paper, a description of *F*-test as a good criterion for implementation of this linear regression typology has been shown. Otherwise, use of SMLR to solve an important physical problem, earthquakes localization, has been shown. Indeed, to establish in a exact way geographical coordinates of a seismic event is very relevant to obtain all the essential information about it. In particular, an essential point is finding geographical coordinates of seismic events which happen on volcanic areas. If these events happen in a tight period of time and their hypocenters are collocated along volcanic pipe, it could possibly be an imminent magma eruption. This is the reason because an application of computing earthquakes localization in Mount Vesuvius by means of SMLR has been shown. Mount Vesuvius is an active volcano which is placed about 9 km east of Naples, Italy: since a population of 3,000,000 people live in its foothills, it is one of more monitoring volcanoes in the world. The entire process to locate specific earthquakes which occurred along Mount Vesuvius crater by means of SMLR technique (or better yet, by means of a software named HYPO71PC based on SMLR technique) has been described. In this paper, this kind of explanation is preceded by a generic overview about earthquakes localization problem and it is followed by a concise description of the applications which have earthquakes localization as starting point.

Corresponding author: Giuseppe Pucciarelli, Ph.D., research fields: geophysics, volcanology and numerical simulation.

2. Statistical Model: The Stepwise Regression

Mathematically speaking, the regression is a statistical process which allows obtaining an estimate

of an assumed value from a dependent variable Y as a function of n independent variables X_1 , ..., X_n. The most common type of regression is the linear one. This is based on the idea that for each sample of observations, there has been a determination of the variable Y and n determinations of the variables X_1 , ..., X_n. The goal is to find a linear relation between these variables. As is well-known, the most simple linear relation is that given by an affine transformation linear that has the Eq. (1):

$$Y_i = \beta_0 + \beta_1 X_1 + \varepsilon_i \quad (1)$$

where i varies between the observations, i.e. $i = 1, ..., n$; Y_i are the dependent variables; X_i are the independent variables, called regressors; $\beta_0 + \beta_1 X_i$ is the regression line, called also regression function; ε_i represents the statistical error.

Eq. (1) has the Eq. (2):

$$Y = \beta_0 + \beta_1 X + \varepsilon \quad (2)$$

in which the vectors Y, X and ε are n-dimensional. The values β_0 and β_1 represent the parameters of the model which have to be estimated by the obtained observation samples (so, they are deterministic); instead, the vector ε contains only stochastic parameters to be determined, because for every assumed value from X, it exists in an entire probability distribution that contains values of Y (for this reason, it is impossible to know with certainty the value of Y). Thus, the relation Eq. (2) gives a random variable, where its probability distribution and characteristics are determined from the values of X and the probability distribution of ε. Among all of the methods of linear regression known, the most used is surely the method of least squares.

The type of linear regression as soon as view is said simple linear regression, because it is available to have only one independent variable. If instead, there are more independent variables that can be used for the determination of the dependent variable Y, we talk about multiple linear regression. In this case, the equation for the previous problem, becomes:

$$Y_i = \beta_0 + \beta_1 X_{1i} + \beta_2 X_{2i} + ... + \beta_k X_{ki} + \varepsilon_i \quad (3)$$

where with respect to Eq. (1), the only change is that the regression line is $\beta_0 + \beta_1 X_{1i} + \beta_2 X_{2i} + ... + \beta_k X_{ki} + \varepsilon_i$. This equation has a matrix form:

$$Y = X\beta + \varepsilon \quad (4)$$

in which X is a $k \times n$ matrix, while the vectors Y, ε are n-dimensional and β is k-dimensional. A type of multiple linear regression very used for the applications in the last years is the so-called stepwise regression [1], discovered from Draper and Smith in 1966 [2]. It is especially used when, in the process of regression, problem is solved by means of independent variables which fail to give information on the variance of the dependent variable: stepwise regression is able to solve this sort of problems. In this method, the total variance is partitioned into two parts: the first one which can be explained by the independent variables (explained variance) and the second one which cannot be explained by them (unexplained variance) [3, 4]. In order to do this, given n indipendent variables X_1, ..., X_n, deemed suitable to the explanation of the variance of the dependent variable, it is possible the extraction step by step (hence the name) of the independent variable that has the highest percentage of the explained variance. Now considering the step $k + 1$: the variabile X_{k+1} is related with X_k of the previous step: thus, Y_k is called residual variable, because it is given by Y minus the linear combination of the independent variables already present in the model. In practice:

$$Y_k = Y - \beta_0 - \beta_1 X_1 - ... \beta_k X_k \quad (5)$$

The variable X_{k+1} introduced in the model will be the one that will show the highest correlation coefficient, in absolute value, with the residual variable. After establishing the criterion for choosing, an algorithm chooses the independent variables suitable for the explanation of the variance of the dependent variable, after an initial setting of a threshold value with which comparing the diffierent correlation coefficients [1, 2]. However, this procedure is not completely reliable (even considering that the threshold value is subjective), therefore the

diffierent correlation coefficients have to satisfy the following null hypothesis:

$$H_0: b_k + 1 \quad (6)$$

where b_k+1 is the so-called regression coefficient, i.e. the slope of a line obtained using linear least squares fitting [5, 6]. So, Eq. (6) affirms that the regression coefficient of the independent variable X_{k+1} to input in the model is zero, after the introductions of $X_1, ..., X_k$. This hypothesis is verified through the F value of Fisher, given by

$$F = \frac{MSR}{MSE} = \frac{\frac{R^2}{k}}{\frac{1 - R^2}{m - k - 1}} \quad (7)$$

in which MSR and MSE are respectively the mean square due to regression and residual; furthermore, the coefficient of determination R^2 is given from:

$$R^2 = 1 - \frac{VAR_{res}}{VAR_{tot}} \quad (8)$$

where the numerator (respectively denominator) is the sample variance of the estimated residuals (respectively dependent variable). It is clear that $0 \leq R^2 \leq 1$ [7].

3. Limits of the Model and Implementation of the Algorithm

The F value of Fischer is based on a single hypothesis: in the stepwise regression, it is hugely violated [7]. As a result, models are too complex and other parameters could be biased towards 0. Therefore, diffierent alternatives for the stepwise regression are developed. The following methods perform better than stepwise, but their use is not appropriate for statistical knowledge [8]: the most important are LASSO, LAR, CROSS VALIDATION and some experimental procedures (not yet enough reliable). Even though no one methods could substitute for statistical experience, LASSO and LAR (especially) are much better than stepwise: these two methods allow us to consider a wide range of options [8]. Through the F value of Fischer, the model with the introduction of the independent variable X_{k+1} is still statistically significant compared to the previous one, which included the independent variables X_1, ..., X_k: this value is also called F to enter. The introduction of new variables could, however, result in an information loss for some variables introduced previously: to check this phenomenon, authors compare the correlation coefficient with another threshold value, known as F to remove: if they are present, these are immediately deleted. Usually, almost all programs have the possibility to follow step by step the regression procedure, through information about the variables and the signalling of F to enter and F to remove which the program utilizes for this particular step. A further option frequently present in the various programs concerns the possibility of choice, on the part of the user, of variables to be introduced or delete in the model: this choice is made through the control of the values of F to enter and F to remove.

4. Earthquakes: The Geiger's Method

Earthquakes' localization constitutes a particular scientific problem where the goal is computing the coordinates of a point situated inside the Earth from which seismic waves are generated. This point is known as the hypocenter of an earthquake and its outside projection is named epicenter. Hypocentral coordinates which authors want to ascertain are four: three are spatial (latitude, longitude and depth) and the other one is the origin time of seismic waves generation. Historically, earthquakes localization was carried out by means of analysis of outside consequences produced by a seismic event. Now, thanks to seismic network development and a more detailed knowledge of interior structure of the Earth, computing of the four earthquakes localization parameters could be done in a more meticulous way. Earthquakes' localization is based on classical linear motion law, that is:

$$x = vt \quad (9)$$

where:

- x is the hypocentral distance, that is the distance between hypocenter and seismic station;
- v represents the seismic waves velocity;
- t is the seismic waves traveltime.

Describing the process in a more practical way, earthquakes localization needs three important features, i.e.:

- knowledge of seismic stations' geographical coordinates;
- picking of seismic phases on seismograms and computing of their traveltimes;
- knowledge of velocity structure between hypocenter and seismic stations.

Therefore, earthquakes' localization is a typical inverse problem, that is a problem in which solution consists in an evaluation of parameters of a determinate model (they must be in good agreement with observations). In this particular situation, parameters are the hypocentral coordinates, while the observations are picked seismic phases and model is an Earth hint between hypocenter and seismic stations. Rewriting Eq. (9) for seismic phases P and S, respectively, that is the first waves generated by a hypocenter which arrive to a seismic station, following equations are obtained:

$$\Delta = v_P(t_P - t_0); \Delta = v_S(t_S - t_0) \tag{10}$$

where Δ is the hypocentral distance, v_P and v_S are the velocities of P wave and S wave respectively, t_P and t_S are the P traveltime and the S traveltime and t_0 is the seismic event origin time. Manipulating in an opportune way Eq. (10), Eq. (11) is obtained:

$$t_S - t_P = \frac{\Delta(v_P - v_S)}{v_P v_S} \tag{11}$$

Replacing Eq. (10) in Eq. (11), Eq. (12) has been obtained:

$$t_S - t_P = \left[\frac{v_P}{v_S} - 1\right] t_P - \left[\frac{v_P}{v_S} - 1\right] t_0 \tag{12}$$

Eq. (12) can be understood as an equation of a line in a cartesian plane where t_P is the abscissa and $(t_S - t_P)$ is the ordinate. In this way, through a simple linear interpolation, parameters can be found. By means of slope, it is possible to compute v_P/v_S , while the y-intercept allows the computation of seismic event origin time t_0. From values of these specific parameters, it is easy to obtain Δ through Eq. (11). Earthquakes' localization can be realised in a graphic way by means of so-called circle method [9]. If at least three seismic stations are at our disposal, for each station the epicentral distance has been computed. Then, a circle with the centre arranged on a seismic station and with radius equivalent to epicentral distance is drawn. The point of intersection among all the circles is the localization of an earthquake. A modification of this method is the following. If only P seismic phases and three stations are computed, circle method is applied in the same way as previously described for two of three stations. In this case, earthquakes' localization is the centre of a circle tangent at two drawn circles and passing through the third remaining seismic station. Both linear interpolation and circle method show us the following set of problems:

- Earth between hypocenter and seismic stations is considered as a homogeneus halfspace where the velocity of seismic waves is constant. Obviously, this is not the real case.
- Earth's depth is completely disregarded.
- Consideration of a spherical Earth is completely disregarded.

In 1912, L. Geiger introduced an algorithm to solve the problem of earthquake localization, considering three criticisms mentioned before. This method, justly called Geiger's method, is still used as basis of software for earthquakes localization [10]. Starting point of this method is model of representing Earth as a sequence of parallel layers where in each one of them, seismic waves velocity is constant. Starting from a trial solution for localization, it is named $m_0(x_0, y_0, z_0, t_0)$. After, there is the procedure of computation

of the so-called residuals. For the *i*-th seismic station, Eq. (13) is defined:

$$R_i = T_i - t_i \quad (13)$$

where R_i is the *i*-th residual that is the simple diffierence between theoretical traveltime T_i and observed (by means of seismograms interpretation) traveltime t_i. Writing T_i in function of m_0, Eq. (13) becomes:

$$R_i = T_0 + \frac{1}{v}[(x_0 - x_i)^2 + (y_0 - y_i)^2 + (z_0 - z_i)^2] - t_i \quad (14)$$

where *v* is the velocity of considered seismic wave.

Now, rewrite Eq. (14) and apply on it an expansion in Taylor series at m_0. In this way, Eq. (14) becomes:

$$R_i \sim R_i(m_o) + a_i \Delta x + b_i \Delta y + c_i \Delta z + \Delta t \quad (15)$$

where $a_i = \frac{\partial R_i}{\partial x_0}$, $b_i = \frac{\partial R_i}{\partial y_0}$, $c_i = \frac{\partial R_i}{\partial z_0}$ with all partial derivatives calculated in m_0 and $\Delta x = x - x_0$, $\Delta y = y - y_0$, $\Delta z = z - z_0$, $\Delta t = t - t_0$.

Finally, a least squares method to make residual minimum is used. Therefore, hypocentral parameters are computed when $\sum_{i=1}^{n} R_i^2$ is minimum with *n* seismic stations.

Summarising, to localize an earthquake, this procedure should be:

(1) Acquisition of seismic phases and of observed traveltimes by means of seismograms.

(2) Geographical coordinates of seismic station which have minimum observed traveltime become spatial coordinates of trial solution m_0. While authors assume as t_0, the P seismic wave traveltime registered at that seismic station deprived of a quantity depending on velocity model authors choose.

(3) Computation of residuals.

(4) Appropriate correction of trial solution.

(5) New computation of residuals.

(6) Repetition of (4) and (5) until when $\sum_{i=1}^{n} R_i^2$ is minimum.

It is appropriate to emphasize how solution's goodness depends on an adequate seismic rays coverage, a sufficient knowledge of velocity model and a careful picking of seismic phases.

5. Application: Examples of Earthquakes Localization on Mount Vesuvius

Mount Vesuvius is an active stratovolcano which is situated about 9 km east of Naples, Italy, and a short distance from the shore. Since a population of 3,000,000 people live in its vicinity, it is one of more monitoring volcanoes in the world. And one of monitoring strategies is earthquakes localization. Indeed, earthquakes localization is very important in volcanic areas because a contingent high concentration of seismic events could be due to magma rising along the volcanic pipe. Magma rising causes a gradual deformation of volcanic pipe rocks which can trigger seismic events. And often magma rising could forerun an eruption. Therefore, accuracy of earthquakes localization in volcanic areas could prove to be fundamental. In this paper, a computed earthquakes localization of 2,315 seismic events which occurred on Mount Vesuvius in a period from 06/12/1986 to 31/12/1999 and was registered by 41 seismic stations belonging to OV-INGV Mount Vesuvius monitoring network is shown. It is important to underline that only P and S seismic phases have been chosen for localization. Starting point is choice of an opportune velocity model to schematise Earth. This last one is a standard 1-D velocity model for Mount Vesuvius area (see Fig. 1) which has already been in other previous works with satisfactory results. This model schematises Earth in a depth interval between 0 and 30 kilometers. Model is composed of six layers and in each of them P wave velocity is assumed to be constant. Then, earthquakes localization is computed by means of HYPO71PC software. This software is a FORTRAN code and it represents one of more sofisticated versions of original code HYPO71PC. Other similar versions are HYPOELLIPSE and HYPOINVERSE. This software

is nowadays widely used for earthquakes localization. The reason for this is the following one. This software makes use of stepwise multiple linear regression to carry out six points of earthquakes localization procedure which have been previously described in Chapter 5. In particular, it carries out the point (6) and it shows lots of benefits in accuracy and convergence of solution. In this particular case, an input file named VESUVIO.PHA is supplied to Hypo71PC. This file is organised in the following way: First of all, it presents the command HEAD followed by the number of characters used to write a heading above each earthquake in the output. This command is put equal to 20. Then, the command RESET is written. This command allows setting values of the software test variables in a way which is straightly connected to input data. In this particular case, seven test variables are test. Among these, the critical *F* value for stepwise multiple regression is set. In Hypo71PC, this value should be included between 0.5 and 2 according to number and quality of available P and S traveltimes. Indeed, if this value is lesser than 0.5, then coefficients matrix of Eq. (15) could be ill-conditioned. Instead, if this value is greater than 2, then Geiger's iteration may finish prematurely and therefore a good localization could be not obtained. For avoiding it, critical *F* value is set equal to 0.5 because there are not lots of available S traveltimes. Then, geographical coordinates (latitude and longitude) of seismic stations which have recorded earthquakes to localize must be written. After the realization of this procedure, velocity model must be choosen. Hypo71PC procures two options: station delay model and variable first layer model. In first case, there is the simple addition or subtraction to traveltimes of a number which is stated for each seismic station. In second one, this stated quantity—previously described—is interpreted as a thickness to add to first layer. Therefore, each seismic station has the same P-wave velocity but thickness of first two layers under each seismic station varies. This typology of model is often chosen when there is the case of different travel paths, that is to say, paths do not come from an uniform reason. Fortunately, this is not the case and therefore station delay model is chosen. Following step is writing a record in which parameters of trial solution and control indicators for the software are indicated. In these parameters of the trial focal depth, the distance from epicenter and others concerning the earthquakes localizations are set (see Ref. [11]). It is important to underline how there are other possible options that can be activated, especially, options concerning geographical coordinates of a trial solution, but this is not the case. Therefore, for each earthquake, Hypo71PC chooses as geographical coordinates of trial solution those of seismic station which is nearest to earthquake localization. Finally, in the last part of input file traveltimes are found. They are organised in the following way. For each earthquake, this is the structure of the script: the acronym of seismic station which has recorded that earthquake, the symbol of analysed seismic phase (that is, P), P-traveltime at that station with accuracy down to centiseconds and, when they have been recorded, S-traveltime at that station with accuracy down to centiseconds. When all traveltimes records regarding to a specific earthquake have been written, then the character "10" in the record immediately following is written. This particular record is considered as a pause between traveltimes of a seismic event and traveltimes of another one. The output file is named VESUVIO.PRT: it is divided into two parts, where in the first one the most important thing is given from the root mean square error of time residuals, that is:

$$RMS = \sqrt{\frac{R_i}{NO}} \tag{16}$$

where R_i is the quantity described in Eq. (14), while *NO* is the number of station readings used in locating the earthquake. The second part of output file is about the characteristics of seismic station: for further information (see Ref. [11]). The result of earthquakes

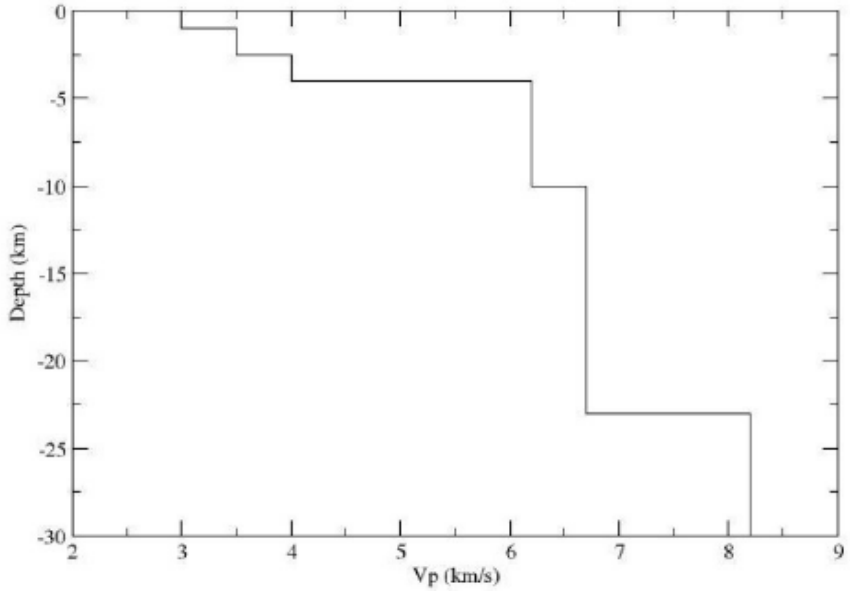

Fig. 1 1D velocity model for Mount Vesuvius area used as input for computing earthquakes localizations.

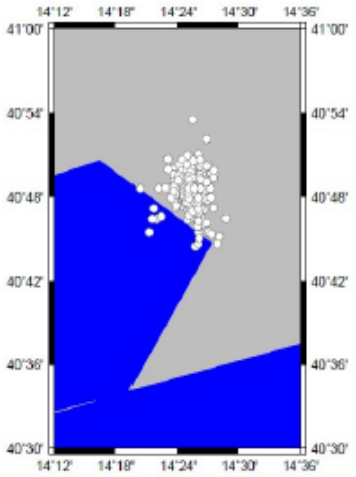

Fig. 2 Earthquake localization in Mount Vesuvius area: the hypocenters are represented by these white circles in the figure.

localization in Mount Vesuvius area is shown in Fig. 2.

6. Conclusions

In this paper, an interesting characteristic of an important topic in statistical field is described: the SMLR. Especially, the aim is to underline a particular link between statistics and physics, explaining how SMLR can be used in the solution of a very important physical problem: the earthquakes localization. Indeed, SMLR is used to implement Geiger's method [10] by means of a subroutine of software HYPO71PC [11, 12]. Its mode operation has been described through a concrete example as computation of some Mount Vesuvius earthquakes localization. Understanding how SMLR could be connected with this relevant physical problem is very important because a good earthquakes localization represents a starting point for other

geophysical research techniques as seismic tomography [13, 14], focal mechanism implementation [15], good resolution of epicentral distance [16] and obtaining of graphical images by means of GMT (Generic Mapping Tools) [17]. Of course, other methods for locating earthquakes exist, for example, Metropolis-Gibbs Method [18]. It is based on a 3D velocity model. This kind of method has already been used to locate earthquakes on Mount Vesuvius [19]. Method which has been described in this paper where SMLR is implemented is based on a 1D velocity model. But 3D velocity model tests have already been carried out [20]. For future studies, development of these 3D velocity model tests using data treated in this paper could be appropriate.

This map is given by the geographical coordinates, i.e. latitude and longitude.

References

[1] Burnham, K. P., and Anderson, D. R. 2002. *Model Selection and Multimodel Inference.* New York: Springer.

[2] Wessel, P., and Smith, W. H. F. 1991. "Free Software Helps Map and Display Data EOS." *Advancing Earth and Space Science* 72 (41): 441-6.

[3] Cohen, J., and Cohen, P. 2010. *Applied Multiple Regression/Correlation Analysis for the Behavioral Sciences*, 2nd edition, Taylor & Francis e-Library.

[4] Chatterjee, S., and Hadi, A. S. 2012. *Regression Analysis by Example*, 5th edition, John Wiley & Sons.

[5] Hansen, P. C., Pereyra, V., and Scherer, G. 2012. *Least Squares Data Fitting with Applications.* Baltimore: Johns Hopkins University Press.

[6] Lawson, C., and Hanson, R. 1987. *Solving Least Squares Problems, Series: Classics in Applied Mathematics*. Book 15, Society for Industrial and Applied Mathematics.

[7] Harrell, F. E. 2001. *Regression Modeling Strategies: With Applications to Linear Models, Logistic Regression, and Survival Analysis*. New York: Springer-Verlag.

[8] Flom, P. L., and Cassell, D. L. 2007. "Stopping Stepwise: Why Stepwise and Similar Selection Methods Are Bad, and What You Should Use." Presented at Northeast SAS Users Group (NESUG) Annual Conference.

[9] Piana Agostinetti, N., and Chiarabba, C. 2008. "Seismic Structure beneath Mt. Vesuvius from Receiver Function Analysis and Local Earthquakes Tomography: Evidences for Location and Geometry of the Magma Chamber." *Geophys. J. Int.* 175 (3): 1298-308.

[10] Geiger, L. 1912. "Probability Method for the Determination of Earthquake Epicenters from Arrival Time Only." *Bulletin St. Louis University* 8: 60-71.

[11] Lee, W. H. K., and Valdes, C. M. 1985. "HYPO71PC: A Personal Computer Version of the HYPO71 Earthquake Location Program." U.S Geological Survey, Open File Report 85749.

[12] Lee, W. H. K., and Lahr, J. C. 1975. *"HYPO71: A Computer Program for Determining Hypocenter, Magnitude and first Motion Pattern of Local Earthquakes*." U. S. Geological Survey, Open File report, pp. 75-311.

[13] Lahr, J. C. 1979. "HYPOELLIPSE: A Computer Program for Determining Hypocenter, Magnitude and first Motion Pattern of Local Earthquakes." U. S. Geological Survey, Open File report, pp. 79-431.

[14] Seber, G. A. F., and Lee, A. J. 2003. *Linear Regression Analysis*, 2nd edition. Hoboken, NJ: John Wiley & Sons.

[15] Labay, A., and Haeussler, P. J. 2007. "3D Visualization of Earthquake Focal Mechanism Using Arcscene." U. S. Geological Survey.

[16] Wallace, T. C., and Lay, T. 1995. *Modern Global Seismology*. San Diego: Academic Press.

[17] Wessel, P., Smith, W. H. F., Scharroo, R., Luis, J. F., and Wobbe, F. 2013. "Generic Mapping Tools: Improved Version Released." *EOS, Transaction AGU* 94: 409-10.

[18] Lomax, A., Virieux, J., Volant, P., and Berge, C. 2000. *Probabilistic Earthquake Location in 3D and Layered Models: Introduction of a Metropolis-Gibbs Method and Comparison with Linear Localizations,* edited by C. H Thurber, N. Rabinowitz, Kluwer, Amsterdam: Advances in Seismic Event Location, pp. 101-34.

[19] Lomax, A., Zollo, A., Capuano, P., and Virieux, J. 2001. "Precise, Absolute Earthquake Location under Somma-Vesuvius Volcano Using a New 3D Velocity Models." *Geophys. J. Int.* 146: 313-31.

[20] Chen, H., Chiu, J. M., Pujol, J., Kwanghee, K., Chen, K. G., Huang, B. S., et al. 2005. "A Simple Algorithm for Local Earthquake Location Using 3D Vp and Vs Models: Test Examples in the Central United States and in Central Eastern Taiwan." *Bull. Seism. Soc. Am.* 96 (1): 288-305.

Journal of Environmental Science and Engineering B 7 (2018) 111-116
doi:10.17265/2162-5263/2018.03.004

Cost Evaluation of Compact Dairy Wastewater Treatment System in Kuwait

Saud Bali Al-Shammari[1] and Noora Abdulmalek[2]

1. Environmental Health Departments, College of Health Science, The Public Authority for Applied Education and Training, Faiha 72853, Kuwait

2. Kuwait Institute for Scientific Research, Water Technologies Department, Safat 13109, Kuwait

Abstract: In Kuwait, wastewater management has gained extra attention in recent years and becomes crucial for sustainable industrial development sector. Among the food industry sector, dairy processing plants generate huge amount of wastewater, which is heavily loaded with organic and other toxic compounds. Disposal of dairy wastewater effluent without sufficient treatment can contaminate aquatic ecosystems. Cost efficient treatment processes that are effective in removing organic load and other contaminants are essential to meet stringent environmental regulations applied in Kuwait. A research study was carried out at the KISR (Kuwait Institute for Scientific Research) to assess the technical viability and economic feasibility of combined microfiltration and biological treatment system. This work presents the economic evaluation of the adopted treatment system. The results show that the cost of the integrated system for large scale is estimated to be US$ 1.575/m^3, which is 25% less than the cost of wastewater transportation and treatment in conventional sewage plants.

Key words: Wastewater, treatment, dairy, cost.

1. Introduction

Dairy industry is very important to state of Kuwait and its products are wildly consumed by Kuwaiti people. Similar to most of food industries, the dairy industry characteristically requires very large quantities of freshwater and generates large quantites of wastewater [1]. Most of the wastewater volume generated in the dairy industry results from cleaning of transport lines and equipment between production cycles, cleaning of tank trucks, washing of milk silos and equipment malfunctions or operational errors [2, 3]. Disposing untreated dairy wastewater can lead to adverse public health and environmental impacts. Examples of environmental concerns include objectionable odors and fly infestations that have resulted from the disposal of the untreated effluent in open land [4]. Recently, the enforcement of environmental legislations is becoming a high priority for the state of Kuwait. Dairy industrial sectors have to comply with the KEPA (Kuwait Environment Public Authority) regulations for wastewater discharge and reuse [5]. To satisfy these regulations the effluent must be collected and treated to meet the quality standards set by KEPA. A research project was conducted to assess the technical viability and economic feasibility of implementing MBR (Membrane Bioreactor System) to treat dairy wastewater effluent generated by one of the largest dairy companies in Kuwait [6]. This work describes the experimental set-up and economic assessment of treating dairy processing wastewater by integrated MBR system.

Corresponding author: Saud Bali Al-Shammari, Ph.D., Associate Professor, research fields: water and wastewater treatment, environmental engineering and seawater desalination.

2. Process Description

The complete system for dairy processing wastewater treatment involves the integration of membrane separation and conventional biological treatment processes. The membrane separation process includes the submerged membrane microfiltration system,

which is a polypropylene membrane filter to remove particles greater than 0.2 μm in size from a feed stream. The main treatment steps in the integrated system are shown in Fig. 1, in which feed water passes through an aeration tank for biological treatment. An air compressor injects adequate air into the aeration tank. The aerobic system includes the process air blowers, which are installed adjacent to the system. The required process airflow is 227 m^3/h introduced at the bottom of the aerobic tank through air scour distribution header pipes. After passing through the upstream flow, the mixed liquor is transferred by overflow to a suitable buffer flow tank and then pressurized to an operating pressure in accordance with the membrane's design.

3. Cost Analysis

In KD-Cow (Kuwait Dairy Company) factory the dairy production process requires huge quantities of freshwater which is used mainly for cleaning purposes and, as a result, large amounts of wastewater are generated. Due to lack of treatment system in the factory, this wastewater is transported and distributed to remote sites through sewage tankers. The company uses 17 sewage tankers per day with a capacity of 30 m^3. The purpose of this study is to evaluate the economic feasibility for the treatment of dairy processing wastewater effluent for reuse. Specifically, the objectives of this task are to:

- To estimate the operating cost and total cost of the dairy wastewater treatment;
- To calculate the unit costs of the treatment of dairy wastewater;
- Use economies of scale to figure out the feasibility of the project.

3.1 Cost Estimation

Table 1 shows experimental plant operating data for the integrated system as obtained during the project. Table 2 provides the estimated cost details for operation expenses.

3.1.1 Capital Costs

Costs incurred on the purchase of land, buildings, construction and equipment to be used in the production of goods or the rendering of services are categorized under capital cost. In other words, it is the total cost needed to bring a project to a commercially operable status. Capital costs do not include labor costs except for the labor used for construction. Unlike operating costs, capital costs are one-time expenses, although payment may be spread out over many years. Capital costs are fixed and are therefore independent of the level of output.

3.1.2 Operation Costs

Total cost needed in daily operations is categorized under operation costs. Operation costs are variable costs, and are dependent on the level of output.

Table 3 shows the total cost calculations for the dairy processing wastewater treatment and expenses details for the operation costs. The total cost is US$ 171,975.

4. Results and Discussion

The estimates of unit costs of the experimental plant for wastewater treatment are provided in Table 4. The estimated unit costs are US$ 2.695/m^3.

In Table 5, the unit costs are represented as percentages of the total unit cost, where capital costs account for approximately 65% of the total cost and operating cost is estimated to be around 35%.

Table 5 shows the estimated unit costs using a small experimental plant operating data. A scale-up approach will be used to determine the cost of a large capacity plant. Due to economies of scale, the unit cost for a larger plant is likely to be lower than in a smaller one. The Eq. (1) will be used to scale-up the unit cost of the pilot plant:

$$C_x = C_y (Q_x/Q_y)^{\eta} \quad (1)$$

where:

C_x = The capital cost for a large plant with a specific capacity;

C_y = The capital cost for a small pilot plant with its actual capacity;

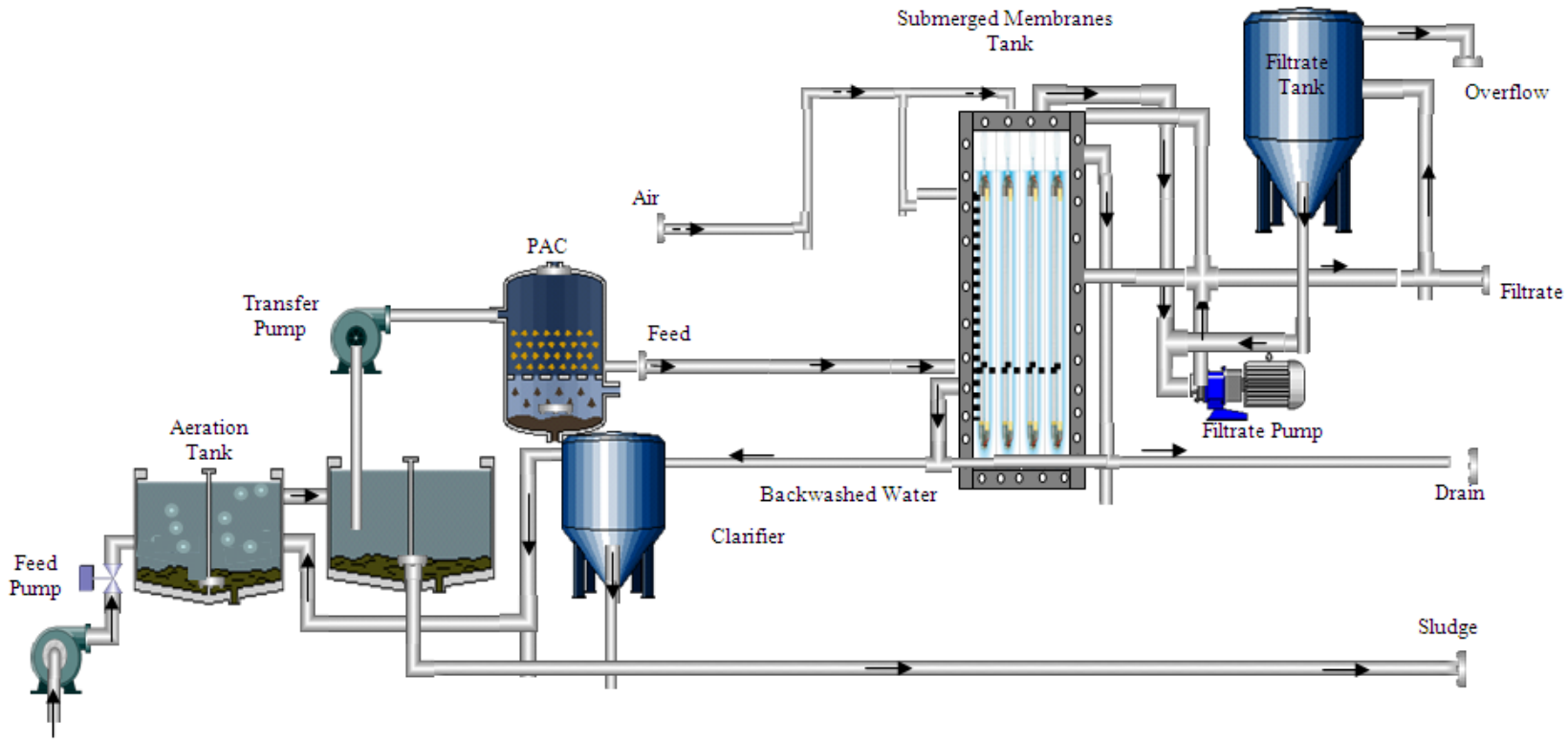

Fig. 1 Integrated submerged membrane microfiltration treatment system.

Table 1 Operating data for the integration system and the experimental plant.

Parameter	Dairy operations
Plant capacity (m^3/day)	24
Plant life (years)	20
Running days	137
Running hours (h)	2,972
Feed inflow (l/h)	1,000
Filtrate outflow (l/h)	1,000
Feed pressure (bar)	1.05
Total feed (m^3)	2,972
Total filtrate (m^3)	2,972
Total electricity consumed (kWh)	27.8

Table 2 Estimated costs of capital and operating expenses.

Parameters	Cost (US $)
Total unit capital cost	95,000
Machinery—compressor	3,000
Machinery—feed pump	1,000
Machinery—transfer pump	900
Machinery—backwash pump	1,000
Tanks	2,830
PVC pipes and valves	540
Membranes	9,260
Civil work	3,330
Concrete base	3,330
Kirby shade	2,660
Operating cost	0.335
Manpower for monitoring (2 technicians)	2,330
Chemicals agent (100 lts)	400
Maintenance and spare parts	1,066

Table 3 Total costs of dairy processing wastewater effluent for reuse.

Capital cost		Cost (US $)
	Machinery—unit cost	95,000
2	Machinery—compressor	12,000
3.	Machinery—feed pump	4,000
4	Machinery—transfer pump	3,600
5	Machinery—backwash pump	4,000
6	Membranes	37,335
7	Tanks (3 tanks)	2,830
8	Manpower	4,665
6	Total civil work	6,000
	Total capital cost	169,165
B.	Operating cost	
1	Electricity = (E/Q)*R	1.65
2	Chemicals	1,200
3	Pipes and valves	545
4	Maintenance and Maintenance parts	1,065
	Total operating cost	2,810
Total cost		171,975

Table 4 Estimates of unit costs for the treatment of wastewater produced from dairy production in a small experimental pilot plant.

Wastewater treatment		Cost (US $)
A	Total unit capital cost (depreciation)	
1	Unit Cost	0.543
2	Machinery—compressor	0.068
3	Machinery—feed pump	0.023
4	Machinery—transfer pump	0.020
5	Machinery—backwash pump	0.023
6	Membranes	0.212
7	Tanks	0.016
8	Manpower	0.811
9	Total civil work	0.034
B	Operation cost	
1	Electricity	0.0006
2	Chemicals	0.403
3	Pipes and valves	0.182
4	Maintenance and maintenance parts	0.359
Total cost (A+ B)		2.695

Table 5 Distribution of unit costs for the treatment of wastewater produced from dairy production in a small experimental pilot plant.

Wastewater treatment		Cost (%)
A	Total unit capital cost (depreciation)	64.90%
1	Unit cost	20.12%
2	Machinery—compressor	2.54%
3	Machinery—feed pump	0.85%
4	Machinery—transfer pump	0.76%
5	Machinery—backwash pump	0.85%
6	Membranes	7.85%
7	Tanks	0.60%
8	Manpower	30.06%
9	Total civil work	1.27%
B	Operation cost	35.10%
1	Electricity	0.02%
2	Chemicals	14.98%
3	Pipes and valves	6.78%
4	Maintenance and maintenance parts	13.32%
Total cost (A+ B)		100%

Table 6 Unit cost estimates for treatment of wastewater produced from dairy production in a large commercial size plant.

Unit cost (US $)	Economies of scale		
	$\eta = 0.95$	$\eta = 0.90$	$\eta = 0.85$
Capital	0.63	0.413	0.270
Operation	0.945	0.945	0.945
Total	1.575	1.355	1.575

Q_x = The capacity of a large plant (120,000 m^3/d);

Q_y = The capacity of a small pilot;

η = A parameter representing economies of scale.

The value of η is unknown due to lack of relevant information. Therefore, different assigned values will be used in this study ($\eta = 0.95$, $\eta = 0.90$ and $\eta = 0.85$)

which imply a modest to reasonable level of economies of scale. Not all cost components are affected to the same degree by plant capacity. The most affected component is the capital cost, so for simplicity, an assumption will be made that no economies of scale exist in other components.

Table 6 shows the variation of the unit cost with different value of η .Whereas the economies of scale increase, the estimated unit cost decreases.

For a modest economies of scale (η = 0.95), the unit cost of the system is estimated to be US$ 1.5/m^3 and for a greater economies of scale (η = 0.85), the unit cost is estimated to be US$ 1.575/m^3.

Currently, 17 tankers with an 30 m^3 capacity are hired to carry the wastewater. The cost of each tanker is US$ 45 per day. So the annual cost for wastewater discharge is a total of US$ 280,000. The total amount of wastewater to be carried for one year is 175,200 m^3 and therefore, the annual cost of transporting generated wastewater is US$ 1.55/m^3. Extra cost needs to be added if the tankers dispose the wastewater into nearby conventional treatment plant. The cost of conventional treatment of municipal wastewater in Kuwait was reported by previous study to be US$ 0.55/m^3 [7]. Therefore, the total cost of this process will be US$ 2.1/m^3.

5. Conclusion

The unit costs of dairy-processing wastewater treatment for a small experimental plant using the integrated system technique have been estimated based on the operational data and cost elements. The result is US$ 2.695/m^3 which, in capital costs account for 65% of the total cost, whereas the operating cost accounts for 35% of the total. Using economies of scale to calculate the unit cost for a large commercial plant, the analysis shows that the unit cost is US$ 1.575/m^3, whereas the unit cost for wastewater transportation and treatment in a conventional plant is US$ 2.1/m^3. This reveals that the proposed treatment system is cost effective and can be used to treat industrial waste effluent.

Acknowledgements

The authors would like to express their gratitude to the Kuwait Foundation for Advancement of Sciences for the partial funding of the project and KD-Cow for their cooperation in conducting this study.

References

[1] Fraga, F. A., García, H. A., Hooijmans, Míguez, C. M., and Brdjanovic D. 2017. “Evaluation of Membrane Bioreactor on Dairy Wastewater Treatment and Reuse in Uruguay.” *International Biodeterioration & Biodegradation* 119: 552-64.

[2] Jyothi, C. S., and Bindu, A. G. 2017. “Feasibility of Anaerobic Fluidized Membrane Bioreactor (AFMBR) in the Treatment of Dairy Wastewater—A Review.” *International Journal of Innovative Research in Science and Engineering* 3 (1): 363-9.

[3] Askaran, K. B., Palmowskiand, L. M., and Watson, B. M. 2003. “Wastewater Reuse and Treatment Options for the Dairy Industry.” *Water Science and Technology* 3: 85-91.

[4] Andrade, L. H. F., Mendes, D. S., Espindola, J. C., and Amaral, C. S. 2015. “Reuse of Dairy Wastewater Treated by Membrane Bioreactor and Nanofiltraion: Technical and Economic Feasibility.” *Brazilian Journal of Chemical Engineering* 32 (3): 735-47.

[5] Environmental Public Authority Kuwait (EPA). 2001. Wastewater Criteria for Disposal State of Kuwait.

[6] Al-Shammari, S. B., Bou-Hamad, S., Al-Saffar, A., Salman, M., and Al-Sairafi, A. 2015. “Treatment of Dairy Wastewater Effluent Using Submerged Membrane Microfiltration System.” *Journal of Environmental Science and Engineering A* 4: 107-18.

[7] Abdel-Jawad, M., Ebrahim, S., Al-Tabtabaei, M., and Al-Shammari, S. 1999. “Advanced Technologies for Municipal Wastewater Purification: Technical and Economic Assessment.” *Desalination* 124: 251-61.

Journal of Environmental Science and Engineering B 7 (2018) 117-122
doi:10.17265/2162-5263/2018.03.005

Estimating the Selfing and Migration of *Luehea divaricata* Populations Based on Genetic Structure Data, Using the EASYPOP Program

Caetano Miguel Lemos Serrote[1], Rosalina Armando Tamele[1], Luciana Samuel Nhantumbo[1] and Lia Rejane Silveira Reiniger[2]

1. Departamento de Silvicultura e Maneio Florestal, Faculdade de Ciências Agrárias, Universidade Lúrio, Unango 3302, Mozambique

2. Departamento de Fitotecnia, Universidade Federal de Santa Maria, Santa Maria RS 97105-900, Brazil

Abstract: Genetic structure data of five populations of the *Luehea divaricata* Mart. & Zucc., forest tree species under development in the Atlantic Forest biome, obtained by microsatellite DNA markers, were used in simulations to study their reproductive and ecological pattern. Different selfing and migration rates were tested, using the observed and expected heterozygosity of 0.55 and 0.67, respectively, obtained through the use of microsatellite markers. Closest values were obtained with the use of selfing rates of 0.3 and migration of 0.2. These results suggest the presence of some self-incompatibility system between these species, which reduces, but does not prevent the self-fertilization. The migration rate contributes to a low genetic differentiation between the populations, making the reproductive mode, responsible for the inbreeding observed in the same populations. Authors suggest continuous monitoring of the genetic variability as a guarantee for the persistence of these populations. The study focus on the importance of using computer simulations to investigate ecologic, reproductive and genetic patterns for forestry populations, thus enabling the application of suitable measures for conservation.

Key words: Computational simulations, conservation biology, inbreeding, heterozygosity.

1. Introduction

The exponential growth of the human population, which has been observed over the last decades, has been accompanied by the destruction of the planet's diverse ecosystems, including forestry. The overexploitation of forest resources and the devastation of forest areas to the expansion of agricultural activities are among the main human activities that have resulted in the destruction and fragmentation of habitats and hence the extinction of forest species [1].

Habitat fragmentation is a phenomenon that consists of the subdivision of an area, geographically isolating members of a certain population into two or more fragments. Depending on the distance between fragments, the reproductive system and distance of dispersion of pollen and seeds, the geographic isolation can result in the reproductive isolation, and consequently restriction in the crossings inside the fragments. In a long term, speciation may occur as members of separate groups can develop different evolutionary mechanisms to the point of no longer being able to cross, even if the gene flow is restored. However, the extinction of the population is most likely, due to the size of the isolates, since in small populations there is a greater performance of genetic drift and a greater occurrence of inbreeding. These events reduce genetic variability and make the population susceptible to the effects of cyclical environmental changes such as the occurrence of pests or diseases, occurrence of frosts or floods [1, 2].

The importance of genetic variability is extensive to the evolutionary success of species, since the

Corresponding author: Caetano Miguel Lemos Serrote, master, research field: genetics.

evolution acts on an existing variability in the population, allowing the natural selection to preserve the individuals better adapted to a wide range of environmental variability [3].

The management of a fragmented population goes through the conservation of its genetic variability that can be accomplished by expanding the areas of its fragments with germplasm that adds genetic variability or by allowing the genetic flow between the fragments. In order to define a priority population for conservation and the conservation method to be adopted, the parameters of the genetic structure must be determined through the use of molecular markers, from which the rate of crosses and the level of genetic flow among its fragments can be estimated [4].

Computational simulations offer more accurate alternatives for the estimation of population genetic parameters, including crossover and gene flow rates. The EASYPOP program [5] was used in the present study to simulate selfing and migration rates from microsatellite markers data obtained from five populations of *Luehea divaricata* Mart. & Zucc. (Malvaceae) forest tree species, under development in a Brazilian area of the Atlantic Forest biome, in order to provide credible information for planning their conservation.

2. Material and Methods

2.1 Research Area

Authors studied five *Luehea divaricata* Mart. & Zucc. (Malvaceae) forest populations located in the Brazilin States of Santa Catarina, Paraná, São Paulo and Minas Gerais (Fig. 1).

2.2 Model Settings

Authors used different selfing (0.1, 0.3 and 0.5) and migration rates (from 0.1 to 0.9, with steps of 0.1) in simulations with the computer program EASYPOP version 2.0.1 [5] to determine those that would result

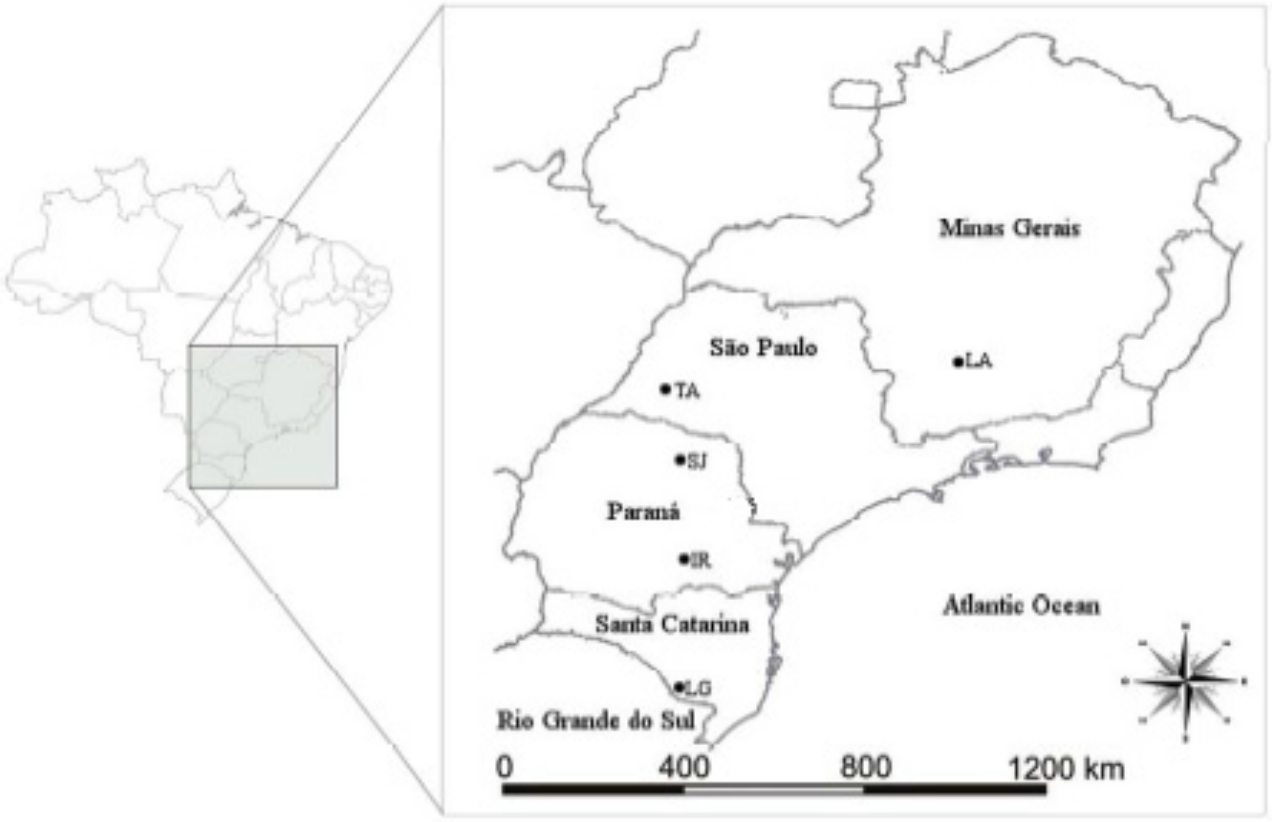

Fig. 1 Geographic location of the five *L. divaricata* populations used in molecular characterization and simulations [6].

Table 1 Values of observed and expected heterozygosities from the five populations used in the study.

Population	State	A	N	Ho	He	F_{IS}
Lages (LG)	SC	2	32	0.64	0.64	-0.01
Irati (IR)	PR	1.3	30	0.65	0.67	0.03
São Jerônimo (SJ)	PR	2.5	30	0.54	0.63	0.15
Taciba (TA)	SP	6.2	28	0.49	0.7	0.31
Lavras (LA)	MG	7.5	30	0.43	0.71	0.40
Average				0.55	0.67	0.88

A: area size, in hectares; N: number of individuals; Ho: observed heterozygosity, obtained by the use of microsatellite markers; He: expected heterozygosity, obtained by the use of microsatellite markers; F_{IS}: inbreeding coefficient. Adapted from Ref. [6].

in parameters similar to those determined by Conson [6] when studying the genetic structure of nine *Luehea divaricata* populations in the Atlantic Forest, in Brazil. In the referred study, the average observed heterozygosity was 0.55, and the average expected heterozygosity was 0.67 (Table 1).

For the simulations, authors considered diploid hermaphrodite specie, with non-random mating and no clonal reproduction. A spatial migration model was considered, with coordinates based on the geographic location of the populations and where obtained from the real geographical coordinates (latitude and longitude) according to the map.

With respect to the mutation settings, authors assumed 10 loci evolving according to the single-step mutation model (SSM), with a proportion of 0.1 K-allele model (KAM) events, under 50 possible allelic states, according to the data obtained by Conson [6]. A mutation rate of 0.0001 mutations per locus per generation was assumed. The genetic variability of the initial population was considered the maximum, and authors simulated 400 generations. For each combination of selfing and migration rates, authors replicated 100 replicates.

The observed and expected heterozygosities (0.55 and 0.67, respectively), from Conson [6] were used to select the model settings that presented values closest to the field observations (Table 1). Authors used the two independent sample *t*-tests at a 5% level of probability to compare the values of observed and expected heterozygosities of the selected model with others.

2.3 FSTAT Analyses

Authors used FSTAT program [7] to analyze the output files of the selected model. Through the use of FSTAT, the forest populations, including allelic richness, genetic diversity, and indices of genetic differentiation among populations were characterized. Authors estimated gene flow by the average number of migrants per generation, based on the proportion of the total genetic variance in a subpopulation (R_{ST}). R_{ST} statistic was used in this study in place of the common F_{ST} statistic because authors used microsatellite loci data that evolve according to step-by-step mutations and is the most indicative estimate for genetic differentiation between populations.

The coefficient of inbreeding within the populations (F_{IS}) was used to estimate the rate of apparent outcrossing (*t*a), given by the equation of Nei and Syakudo [8]:

$$t_a = \frac{1 - Fis}{1 + Fis} \quad (1)$$

In turn, authors estimated gene flow in terms of the average number of migrants per generation (*N*m) from the value of R_{ST} [9]:

$$Nm = \frac{1}{4}\left(\frac{1}{R_{ST}} - 1\right) \quad (2)$$

3. Results and Discussion

3.1 Selection of Model Parameters

Values of observed (Ho) and expected (He) heterozygosities generated from EASYPOP simulations for different selfing and migration rates are

Table 2 Estimates of observed (H_O) and expected (He) heterozygosities generated by simulations, for different rates of selfing and migration

Migration rate	Rate of selfing					
	0.1		0.3		0.5	
	Ho	He	Ho	He	Ho	He
0.1	0.656	0.694	0.543	0.658	0.424	0.633
0.2	0.668	0.706	0.555	0.674	0.433	0.647
0.3	0.670	0.708	0.565	0.684	0.433	0.649
0.4	0.674	0.711	0.568	0.686	0.437	0.653
0.5	0.681	0.719	0.571	0.692	0.441	0.659
0.6	0.683	0.719	0.573	0.695	0.442	0.663
0.7	0.684	0.722	0.575	0.698	0.444	0.664
0.8	0.687	0.723	0.578	0.701	0.446	0.670
0.9	0.689	0.725	0.580	0.705	0.452	0.674

presented in Table 2. There is clear trend of increasing heterozygosity (both Ho and He) with increasing migration rate and reducing selfing. Heterozygosity is one of the parameters of genetic variability. According to Madsen et al. [10], gene flow enables the allele exchange between populations, thus increasing the genetic variability. In turn, selfing limits the pollen and seed dispersion and the potential for recombination between alleles from different individuals; as a result, autogam species tend to present low variability within populations and high variability between populations [11].

The closest values of Ho and He to those obtained through the use of microsatellite markers (0.55 and 0.67, respectively) were generated under the selfing of 0.3 and the migration rate of 0.2 and these values were significantly different from the other rates, based on two independent sample *t*-tests at a 5% level of probability of error. This model enables to characterize the populations.

3.2 Genetic Structure of the Forest Populations

The rate of selfing of 0.3 generated from simulations implies an outcrossing rate of 0.7. This value is in accordance with the apparent outcrossing (*t*a) of 0.696 obtained by using Eq. (2), given the intra-population inbreeding coefficient (F_{IS}) of 0.179 generated from the FSTAT analysis. This finding enables us to classify the mode of reproduction of the population as mixed, with a predominance of outcrossing, according to the classification of Destro and Montalván [12]. This author classifies populations as autogamous (outcross from 0 to 0.05), mixed (outcross from 0.05 to 0.95) and allogamous (outcross from 0.95 to 1.0).

Mixed reproduction system in hermaphrodite vegetal species, like *Luehea divaricata*, suggests the presence of self-incompatibility mechanism in vegetal species that reduce, but do not completely prevent selfing [13]. According to Bawa [14], self-incompatibility is frequently used by angiosperms to prevent the adverse effects of inbreeding and the subsequent loss of genetic variability. Studying *Ceiba aesculifolia* populations, Quesada, et al. [15] observed outcrossing rates close to 1.0 because of a self-incompatibility mechanism present in this species.

With respect to the migration settings, the simulations derived a rate of 0.2 between populations, which is enough to prevent high genetic differentiation between (R_{ST} = 0.0062, from the FSTAT analyze). For gene flow, in terms of *Nm*, the number of migrants per generation, determined through the use of Eq. (3), was 40. This is a high value according to the scale set by Govindaraju [16], which distinguishes the following levels for gene flow: high ($Nm > 1$), intermediate ($0.25 < Nm < 0.99$), and low ($Nm < 0.25$).

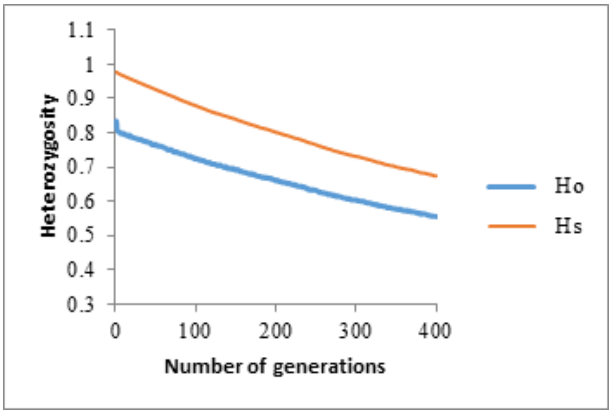

Fig. 2 Simulation of observed (Ho) and expected (Hs) heterozygosities across 400 generations in five populations of *Luehea divaricata*.

Gene flow is the movement of genes (gametes, propagules, and individuals) in populations that effectively changes the spatial distributions thereof. High rates of gene flow result in low genetic differentiation between populations by opposing the effects of evolutionary forces (inbreeding and genetic drift) [17]. A study regarding genetic structure for *Luehea divaricata* in Brazil [9] showed high genetic differentiation (F_{ST} = 0.22) between populations, due to low gene flow. According to Neigel [17], gene flow is an evolutionary force opposite to genetic drift, acting toward the homogenizing allele frequencies between populations, thus resulting in low genetic differentiation between them.

The behavior of observed and expected heterozygosity were plotted across the 400 generations simulated (Fig. 2). High levels of heterozygosities were observed (values close to one) in the beginning, with a progressive loss generation by generation.

Diversity loss may occur due to inbreeding, despite the self-incompatibility mechanisms present in this species. As a result of genetic drift effects, some alleles may lose every generation, including those for self-incompatibility. Inbreeding can also occur from biparental crossings when population size is small. According to Ridley [18], while a great habitat area may have sustained a single great population, it is possible that none of its fragments is able to sustain enough a subpopulation for a long time.

3.3 Implications for Conservation

Forest habitats have been destroyed and fragmented due to anthropic activities that turn a great and continuous area into two or more small sized fragments. In this condition, ecologic and genetic processes may occur and lead to disastrous consequences [1, 2]. Forest fragmentation affects the phenology, pollination patterns and reproductive success of species [2]. The reduction on the population size may reduce the density of reproductive trees and limit pollen availability, and propitiate the occurrence of inbreeding and genetic drift effects that lead to progressive loss of genetic variability and, ultimately, the population extinction.

The findings in this study suggest five genetically stable populations with moderate losses of variability due to high rates of gene flow between them despite high selfing rates. Gene flow enables sharing alleles from different populations and increases the heterozygosity. In order to maintain the present scenario in the future, authors suggest keeping monitoring the genetic variability as a guarantee for the persistence of these populations.

4. Conclusion

The five populations of *Luehea divaricata* present moderate levels of inbreeding as a result of the reproductive mode in this species. However, high rates of gene flow between populations minimize the losses of genetic variability.

This study stressed the importance of using computer simulations to investigate ecologic, reproductive and genetic patterns for forestry populations, thus enabling the application of suitable measures for conservation.

Acknowledgments

This research was supported by Conselho Nacional de Desenvolvimento Científico e Tecnológico (CNPq), Brazil. Authors would like to thank Mr. Basin Alhassan from Ehime University for English language editing.

References

[1] Primack, R. B., and Rodrigues, E. 2001. *Biologia da conservação*. Londrina: Planta.

[2] Alter, S. E., Rynes, E., and Palumbi, S. R. 2007. "DNA Evidence for Historic Population Size and Past Ecosystem Impacts of Gray Whales." *Proceedings of the National Academy of Sciences* 104 (38): 15162-7. doi.org/10.1073/pnas.0706056104.

[3] Silva, S. M. M., et al. 2014. "Prâmetros genéticos para a conservação de *Hymenaea courbaril* L. na Amazônia Sul-Ocidental." *Ciência Florestal* 24 (1): 87-95. dx.doi.org/10.5902/1980509813326.

[4] Sork, V. L., Nason, J., Campbell, D. R., and Fernández, J. F. 1999. "Landscape Approaches to Historical and Contemporary Gene Flow in Plants." *Trends in Ecology and Evolution* 14 (6): 219-24.

[5] Balloux, F. 2001. "EASYPOP (Version 1.7): A Computer Program for the Simulation of Population Genetics." *Journal of Heredity* 92 (3): 301-2. doi.org/10.1093/jhered/92.3.301.

[6] Conson, A. R. O. 2012. "Estrutura Genética em Populações de *Luehea divaricata* Mart. (Malvaceae)." MSc thesis, Universidade Estadual de Londrina.

[7] Goudet, J. 1995. "FSTAT (Version 1.2): A Computer Program to Calculate F-Statistics." *The Journal of Heredity* 86 (6): 485-6. doi.org/10.1093/oxfordjournals.jhered.a111627.

[8] Nei, M., and Syakudo, K. 1958. "The Estimation of Outcrossing in Natural Populations." *The Japanese Journal of Genetics* 33: 46-51. doi.org/10.1266/jjg.33.46.

[9] Nagel, J. C., Ceconi, D. E., Poletto, I., and Stefenon, V. M. 2015. "Historical Gene Flow within and among Populations of *Luehea divaricata* in the Brazilian Pampa." *Genetica* 143 (3): 317-29.

[10] Madsen, T., Stille, B., and Shine, R. 1995. "Inbreeding Depression in an Isolated Population of Adders *Vipera berus*." *Biological Conservation* 75: 113-8. doi.org/10.1016/0006-3207(95)00067-4.

[11] Loveless, M. D., and Hamrick, J. L. 1987. "Distribuicion de la variacion en species de arboles tropicales." *Revista Biologia Tropicales* 35 (1): 165-75.

[12] Destro, D., and Montalván, R. 1999. *Melhoramento Genético de Plantas*. Londrina: Ed. UEL.

[13] Carvalho, P. E. R. 2008. *Espécies arbóreas brasileiras*. Brasília: Embrapa Informação Tecnológica.

[14] Bawa, K. S. 1974. "Breeding Systems of Tree Species of a Lowland Tropical Community." *Evolution* 28 (1): 95-2. doi: 10.1111/j.1558-5646.1974.tb00729.x.

[15] Quesada, M., Herrerías-Diego, Y., Lobo, J. A., Sánchez-Montoya, G., Rosas, F., and Aguilar, R. 2013. "Long-Term Effects of Habitat Fragmentation on Mating Patterns and Gene Flow of a Tropical Dry Forest Tree, *Ceiba aesculifolia* (Malvaceae: *Bombacoideae*)." *American Journal of Botany* 100 (6): 1095-101. doi: 10.3732/ajb.1200542.

[16] Govindaraju, D. R. 1989. "Variation in Gene Flow Levels among Predominantly Self-pollinated Plants." *Journal of Evolutionary Biology* 2 (3): 173-81. doi.org/10.1046/j.1420-9101.1989.2030173.x.

[17] Neigel, J. E. 1997. "A Comparison of Alternative Strategies for Estimating Gene Flow from Genetic Markers." *Annual Review of Ecology and Systematics* 28 (1): 105-28. doi.org/10.1146/annurev.ecolsys.28.1.105.

[18] Ridley, M. 2006. *Evolução*. Porto Alegre: Artmed.

Journal of Environmental Science and Engineering B
Volume 7, Number 3, March 2018

David Publishing Company
616 Corporate Way, Suite 2-4876, Valley Cottage, NY 10989, USA
Tel: 1-323-984-7526, 323-410-1082; Fax: 1-323-984-7374, 323-908-0457
http://www.davidpublisher.com, www.davidpublisher.org
environmental@davidpublishing.com, environmental@davidpublishing.org

ISSN 2162-5263